ELSEVIER

Geoderma 82 (1998) 137–172

GEODERMA

Stable carbon and oxygen isotopes in Quaternary soil carbonates as indicators of ecogeomorphic changes in the northern Chihuahuan Desert, USA

H.C. Monger [a,*], D.R. Cole [b], J.W. Gish [c], T.H. Giordano [d]

[a] *Agronomy and Horticulture, New Mexico State University, Las Cruces, NM 88003, USA*
[b] *Chemical and Analytical Science Division, Oak Ridge National Laboratory, Box 2008, Oak Ridge, TN 37831, USA*
[c] *Quaternary Palynology Research, Rio Rancho, NM 87124, USA*
[d] *Geological Sciences, New Mexico State University, Las Cruces, NM 88003, USA*

Accepted 15 April 1997

Abstract

Stable carbon and oxygen isotopes in soil carbonates provide an additional technique for investigating Quaternary ecogeomorphic changes in arid and semiarid regions. This study presents $\delta^{13}C$ and $\delta^{18}O$ values in surface and buried soils in a Basin and Range region of southern New Mexico and west Texas. Three landform categories were investigated for their isotopic content: (1) middle piedmont slopes; (2) a lower piedmont slope and adjacent playa depressions; and (3) an intermontane basin floor. Soils of the middle piedmont slopes had greatest $\delta^{13}C$ variability, ranging from −0.6‰ in buried soils to −11.1‰ (PDB) in surface soils. Soils of the basin floor had greatest variability in $\delta^{18}O$ values, ranging from −0.6‰ to −7.6‰ (PDB). Fossil pollen patterns roughly paralleled $\delta^{13}C$ shifts, with Cheno-Am pollen exhibiting greatest changes. Both isotope and pollen data across stratigraphic discontinuities suggest that a conversion from C_4 grasses to C_3 desert shrubs accompanied Holocene erosion. © 1998 Elsevier Science B.V.

Keywords: stable isotopes; pedogenic carbonates; paleosols; paleoclimate; desert; soils

1. Introduction

Arid and semiarid environments record paleoclimatic information in several forms: (1) timing of erosion–sedimentation events (Hawley et al., 1976; Bull,

* Corresponding author. Tel.: +1 (505) 646-1910; fax: +1 (505) 646-6041; e-mail: cmonger@nmsu.edu

PII S0016-7061(97)00100-6

1991; Dorn, 1994); (2) fossil pollen (Gish, 1979; Hall, 1985; Horowitz, 1992); (3) packrat middens (Betancourt et al., 1990; Spaulding, 1991); and (4) pluvial lakes (Waters, 1989; Hawley, 1993). More recently, stable isotopes in soil carbonates have emerged as an important paleoenvironmental indicator, where $^{13}C/^{12}C$ and $^{18}O/^{16}O$ ratios provide information about floral communities and climatic parameters (Cerling, 1984; Amundson et al., 1989, 1996; Quade et al., 1989a; Kelly et al., 1993; Nordt et al., 1996; Wang et al., 1996).

Stable isotope values reported in this paper are from a study located on the Fort Bliss Military Reservation in the northern Chihuahuan Desert (Fig. 1). Fort Bliss borders the U.S.D.A. Desert Soil–Geomorphology Project (Hawley, 1975b) to the west and the White Sands Missile Range to the north. Buried soils in this Basin and Range setting occur on piedmont slopes, playa depressions, and the basin floor. Many buried soils are beneath the zone of modern carbonate accumulation, approximately 15 to 45 cm (Gile et al., 1966), and well above groundwater, which is mostly deeper than 40 m (King and Hawley, 1975; McLean, 1975).

In the Chihuahuan Desert, vegetation occurs as mosaics of C_4 grassland and C_3 desert shrub communities (Syvertsen et al., 1976). Carbon isotopes in pedogenic carbonates record vegetation dynamics because carbonate $\delta^{13}C$ values are enriched 14 to 16‰ with respect to the vegetation controlling soil CO_2 (Cerling, 1984; Cerling et al., 1989). If carbonate precipitates in isotopic equilibrium with CO_2 respired by a C_4 desert grassland, for example, the

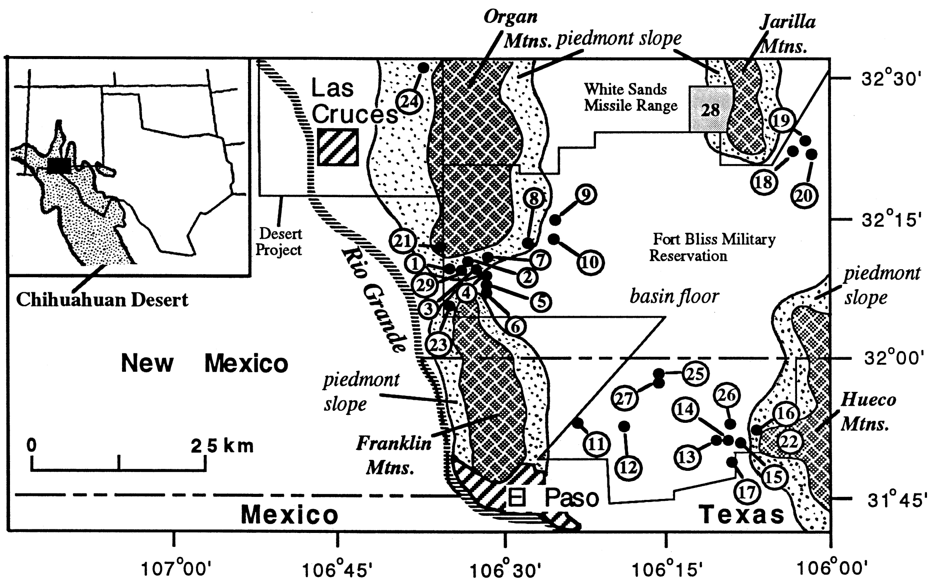

Fig. 1. Map locating Chihuahuan Desert, study area (black rectangle in map insert), and sample locations listed in Table 2.

carbonate should have a $\delta^{13}C$ value of 2‰. In contrast, if carbonate precipitates in isotopic equilibrium with CO_2 respired by a C_3 shrubland, the carbonate should have a $\delta^{13}C$ value of −12‰ (Boutton, 1991). Additionally, the $\delta^{18}O$ content in pedogenic carbonate may contain information about climate change because $\delta^{18}O$ signatures are inherited from rain $\delta^{18}O$ signatures combined with any fractionation in soil (Cerling, 1984; Cerling and Quade, 1993; Liu et al., 1995; Amundson et al., 1996).

Soil carbonates are abundant in soils of southern New Mexico and have been the subject of numerous studies (Gile, 1961, 1995; Gile et al., 1966; Ruhe, 1967; Gile and Grossman, 1979; Gardner, 1984; Schlesinger et al., 1989; Monger and Daugherty, 1991a,b; Monger et al., 1991a,b; Grossman et al., 1995). Paleoenvironmental data in the study area have been generated from soil stratigraphy (Gile, 1975; Hawley, 1975a), fossil pollen (Freeman, 1972), and packrat middens (Van Devender, 1990). The purpose of this paper is to report stable carbon and oxygen isotopic values in pedogenic carbonates occurring across stratigraphic discontinuities and across landforms, and interpret these data in light of pollen and packrat midden paleoenvironmental reconstructions.

2. Geomorphic and ecologic setting

The Chihuahuan Desert is one of North America's largest deserts, extending from New Mexico southward into central Mexico (Schmidt, 1979) (Fig. 1). This region is in the Basin and Range Province dominated by block-faulted mountains of various igneous and sedimentary rocks that are separated by basins filled with Quaternary and Tertiary alluvium (Fenneman, 1931; Seager et al., 1987).

Sample sites in the study area (Fig. 1) occur in three landforms: piedmont slopes, basin floor, and small tectonically produced depressions, or playas, that occupy a narrow zone between the lower piedmont slope and the basin floor (Seager et al., 1987). The piedmont slope is the alluvial region that is bound by mountain bedrock at its upper boundary and the basin floor at its lower boundary (Gile et al., 1981; Peterson, 1981). The piedmont slope of the Organ Mountains is composed of igneous alluvium, in contrast to the piedmont slopes of the Hueco and Franklin Mountains that are composed of limestone alluvium. Soil–geomorphic mapping of Fort Bliss revealed at least seven geomorphic surfaces bound by discontinuities (Monger, 1993, 1995). Geomorphic surfaces on the middle and upper piedmont slopes generally occur as a stepped sequence of surfaces, where older surfaces are topographically higher (Fig. 2). This configuration concentrates water and sediment into inter-fan valleys. In the lower piedmont region, fans coalesce and create a setting where younger surfaces are topographically higher and bury older surfaces (Seager, 1981). Sediments from highest mountain bedrock sources are about 1150 m higher than the lowest elevations in the playa depressions. Peterson (1981) describes similar

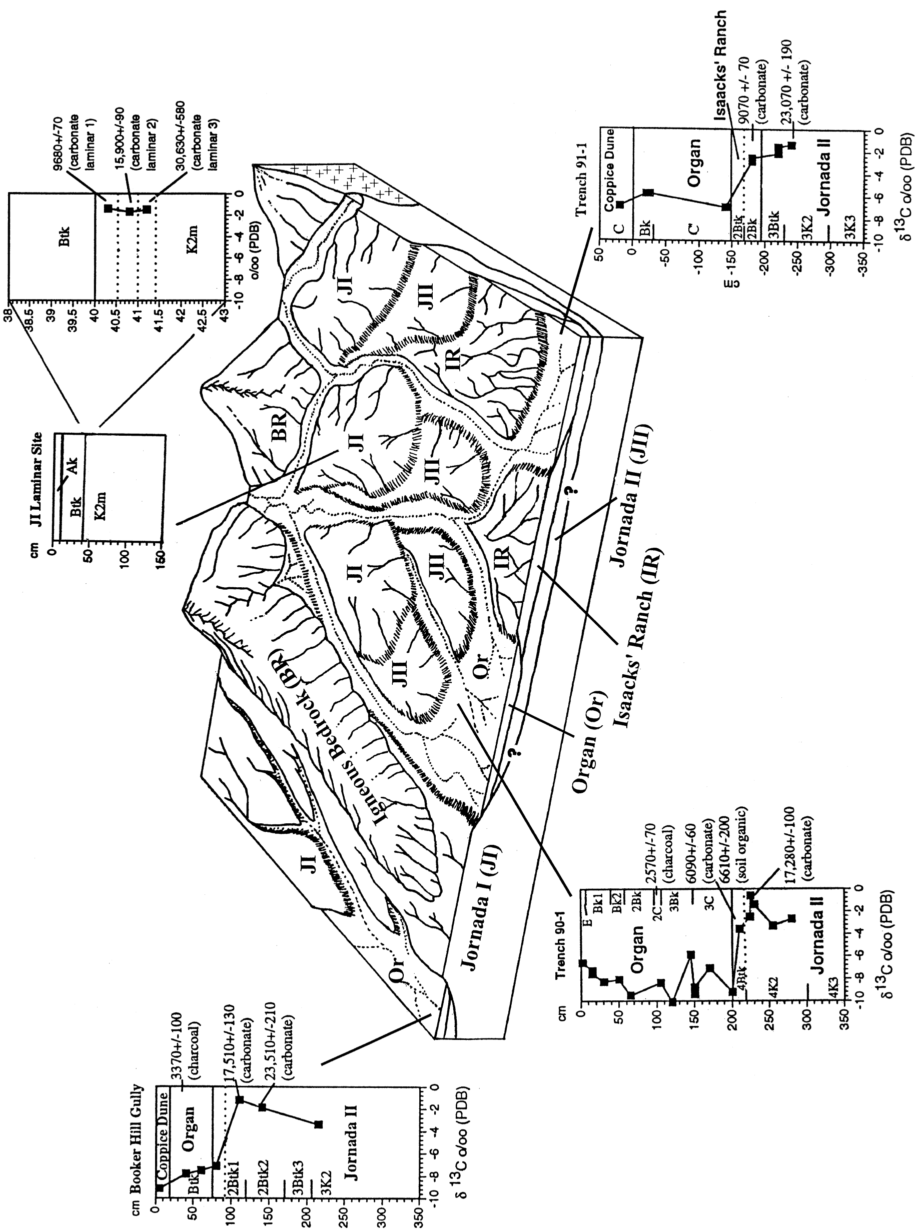
JI Laminae
Btk
K2m
9680+/-70 (carbonate laminar 1)
15,900+/-90 (carbonate laminar 2)
30,630+/-580 (carbonate laminar 3)
o/oo (PDB)
JI Laminar Site
Ak
Btk
K2m
Trench 91-1
Coppice Dune
Organ
Isaacks' Ranch
9070 +/- 70 (carbonate)
23,070 +/- 190 (carbonate)
Jornada II
δ13C o/oo (PDB)
Trench 90-1
2570+/-70 (charcoal)
6090+/-60 (carbonate)
6610+/-200 (soil organic)
17,280+/-100 (carbonate)
Organ
Jornada II
δ13C o/oo (PDB)
Booker Hill Gully
Coppice Dune
Organ
3370+/-100 (charcoal)
17,510+/-130 (carbonate)
23,510+/-210 (carbonate)
Jornada II
δ 13C o/oo (PDB)
Igneous Bedrock (BR)
Jornada I (JI)
Jornada II (JII)
Isaacks' Ranch (IR)
Organ (Or)

relationships of inset and buried surfaces for other piedmont slopes in the Basin and Range.

Ecologically, the Chihuahuan Desert is characterized by contiguous ranges of creosotebush (*Larrea tridentata*) and tarbush (*Flourensia cernua*) (Dick-Peddie, 1993). Grasslands are also common in the Chihuahuan Desert, although their extent has greatly diminished in the last 100 years (York and Dick-Peddie, 1969). The grasslands are dominated by C_4 species, such as black grama (*Bouteloua eriopoda*), mesa dropseed (*Sporobolus flexuosus*), and red threeawn (*Aristida purpurea*). In contrast, shrubs in the Chihuahuan Desert are mainly C_3, such as creosotebush (*Larrea tridentata*), honey mesquite (*Prosopis glandulosa*), and tarbush (*Flourensia cernua*), with the exception of fourwing saltbush (*Artriplex canescens*) which is C_4 (Syvertsen et al., 1976). In the higher elevations, C_3 plants again become dominant, such as red-berry juniper (*Juniperus erythrocarpa*) and Mexican pinyon pine (*Pinus cembroides*) (Allred, 1988). The isotopic signature of rain in the study area has a mean $\delta^{18}O$ value of about $-4‰$ (SMOW) based on interpolation between the contours of the IAEA–WMO network compiled by Yurtsever and Gat (1981).

3. Methods

Geomorphic surfaces on Fort Bliss were identified using topographic relations and soils (Monger, 1993, 1995). Quaternary units used in this study are termed *allostratigraphic units*, which are mapping units that combine geomorphic surfaces with their soils (Peterson et al., 1995). The criteria for the seven allostratigraphic units in this study are listed in Table 1. Table 2 lists pedons, soil horizons, stable isotopic values, and radiocarbon information. Soil horizons were described using the nomenclature of Guthrie and Witty (1982), with the exception of the K-horizon terminology of Gile et al. (1965). Soil carbonate morphogenetic stages follow (Gile et al., 1966). The carbonate morphogenetic stages and allostratigraphic units are displayed in Figs. 3–5.

Pedons in this study were placed into one of three categories: (1) the middle piedmont slope, (2) the lower piedmont slope and tectonic playa depressions, or (3) the basin floor. Soils of the upper piedmont slope were off limits due to military activity. The boundary between the lower piedmont slope and tectonic

Fig. 2. Schematic diagram of the southeastern middle piedmont slope of the Organ Mountains. The diagrams illustrates soil stratigraphy and pronounced $\delta^{13}C$ shift across discontinuities separating Organ sediments from underlying paleosols. The sources of Organ sediments are from erosion of adjacent soils of older surfaces and soils eroded from upslope sources, including mountain bedrock. Also illustrated is the relict Jornada I soil, in which carbonate accumulates as accretionary laminae atop a petrocalcic horizon (K2m).

Table 1
Names and mapping criteria for allostratigraphic units in study area (after Ruhe, 1967; Hawley and Kottlowski, 1969; Hawley, 1975a; Gile and Grossman, 1979; Seager, 1981; Gile et al., 1981)[a]

Allostratigraphic units (landform)	Diagnostic features
Organ (piedmont slope) (eolian basin floor)	Stage I. No or weak argillic; surface graded near modern arroyo system; uppermost stratum in alluvial or eolian aggradational environments; contains charcoal with ^{14}C ages of 6400 ± 110 years B.P. and younger.
Lake Tank (playa depression)	Stage I. No or weak argillic; highest stratigraphic position; depressional equivalent of Organ surface.
Isaacks' Ranch (piedmont slope)	Stage II. Weak to moderate argillic;stepped surface immediately above Organ surface.
Jornada II (piedmont slope)	Stage II to incipient IV. Moderate to strong argillic; stepped surface above Isaacks' Ranch.
Petts Tank (playa depression)	Stage II–III. Moderate to strong argillic; depressional equivalent of Jornada II.
Jornada I (piedmont slope)	Stage III–IV. Strong argillic; highest fan surface in study area; weathered boulders; contains Bishop ash (740,000 years B.P.) and Lava Creek B ash (620,000 years B.P.).
La Mesa (basin floor)	Stage III–V. Formed in fluvial facies of ancestral Rio Grande mostly between the end of the Jaramillo subchron (900,000 years B.P.) and the Matuyama–Brunhes boundary (780,000 years B.P.); overlies several deposits of pumice, the youngest being 1,300,000 years B.P.

[a] Charcoal dates of Organ soils are from Gile (1975). Volcanic ash, paleomagnetic, and pumice dates of Jornada I and La Mesa soils are from Mack et al. (1993, 1996).

depressions is diffuse. Both landforms have fine-textured soils, receive runoff as sheet flow and support denser vegetation than either the middle piedmont slope or basin floor. For these reasons, the lower piedmont slope and playa depression landforms were grouped into one category. Basin floor soils have loamy sand and sandy loam textures and occur primarily as coppice dunes and sand sheets disconformably overlying paleosols. Coppice dunes in the region generally began forming within the last 150 years (Gile, 1966).

Isotope samples from pedons listed in Table 2 were collected in zones of approximately 10 cm, with the exception of five pedons: 90-2, 90-3, 90-4, 90-5, and 91-4, which comprise the soil horizon thickness as listed in Table 2. A variety of carbonate morphogenetic stages, from stage I to stage IV, were analyzed for stable isotopic content (Figs. 3–5). All stage I samples were carbonate filaments. Even in gravelly soils, filaments in the fine earth between clasts were analyzed rather than clasts coatings. This method prevented the sampling of older carbonate coatings, which can be seen on many clasts moving in the modern arroyo system. Once collected, the carbonate filaments were concentrated by sieving with a 53 μm sieve to remove much of the silicate detritus. Stage I filaments from site 14 were concentrated with a micro-siphoning apparatus.

All stage II samples analyzed in this study occurred as carbonate nodules. Nodules within the 10 cm sampling interval were hand-picked and placed in a container. In the lab, nodules were disaggregated with a porcelain mortar and pestle and sieved with a 53 μm sieve. Likewise, all stage III and stage IV samples were disaggregated and sieved. Stage IV laminae atop petrocalcic horizons at sites 7 and 15 were dissected with a small chisel.

Stable isotope analysis was conducted on the disaggregated, sieved material. Samples from the middle piedmont slopes and lower piedmont slope–playa depressions were analyzed at the Oak Ridge National Laboratory, with the exception of that of site 16 that was analyzed at New Mexico Tech University. In both labs, soil carbonate was converted to CO_2 by treatment with 100% phosphoric acid. The CO_2 was purified and its $^{13}C/^{12}C$ and $^{18}O/^{16}O$ ratios were determined by mass spectrometry and reported in standard δ notation relative to the Pee Dee belemnite standard.

Stable isotopic analysis of basin floor samples were conducted on samples also analyzed for ^{14}C ages by Beta Analytic, Inc. In pedon 90-1, ^{14}C ages of both the bulk soil organic carbon and carbonate were measured on the same sample by Beta Analytic, Inc. (Table 2). In some cases, splits of the same sample were sent to different labs. These results are indicated in Figs. 3 and 4 for sites 8, 16, 3, 4, 5, 6, and 9.

Palynological analyses were conducted on nine pedons, of which three contained pollen sufficiently preserved for complete profile characterization (Gish, 1993). Pollen samples were obtained by digging into the profile surface and taking a sample with a trowel cleaned with deionized water between each sample. All samples were sent to the Texas A&M University Palynology Laboratory for standard treatments with hydrochloric and hydrofluoric acid, heavy liquid flotation, and tracer spore addition. Pollen identification was made at Quaternary Palynology Research, Rio Rancho, New Mexico.

4. Results

4.1. Isotopic shifts across discontinuities and landforms

The most obvious $\delta^{13}C$ shifts are on the middle piedmont slope at discontinuities between Organ alluvium and underlying paleosols (Fig. 2). This shift ranges from a high of -0.6 at site 2 to a low of $-11.1‰$ at site 16 (Fig. 3). In

Table 2
Site numbers, site names in parentheses, soil horizon designation and corresponding depths in parentheses, stable isotope values, radiocarbon ages, dated material, and lab identification numbers

Site (name)	Horizon (cm)	δ^{13}C (PDB)	δ^{18}O (PDB)	^{14}C age years B.P.	Dated material	Lab. No.
1 (BHG)	C (5)	−9.1	−6.3			
	Btk 1 (40)	−7.8	−5.3	3,370 ± 100	charcoal	Beta-51876
	Btk2 (60)	−7.5	−5.1			
	2Btk1 (80)	−7.1	−5.3			
	2Btk2 (110)	−1.2	−5.3	17,510 ± 130	carbonate	Beta-55374
	3Btk3 (140)	−1.9	−5.9	23,510 ± 210	carbonate	Beta-55375
	3K3 (215)	−3.4	−6.1			
2 (90-1)	E (2)	−6.6	−5.1			
	Bk1 (15)	−7.3	−5.2			
	Bk1 (15)	−7.6	−5.8			
	Bk1 (30)	−8.3	−4.5			
	Bk2 (50)	−8.1	−4.2			
	2Bk (65)	−9.5	−5.2			
	2C (105)	−8.4	−4.9	2,570 ± 70	charcoal	Beta-47196
	2C (105)	−25(OC)				
	3Bk (120)	−10.1	−6.1			
	3Bk (120)	−25(OC)				
	3Bk (145)	−5.9	−4.4			
	4Btk (150)	−9.4	−5.9			
	4Btk (150)	−23.5 (OC)				
	4Btk (150)	−8.8	−5.6			
	4Btk (150)	−24.5 (OC)				
	3C (170)	−7.1	−5.8			
	4Btk (200)	−9.2	−4.9			
	4Btk (210)	−3.6	−7.2	6,090 ± 60	carbonate	Beta-74116
	4Btk (210)	−19.2		6,640 ± 200	bulk soil organic	Beta-74115

	4K2m (224)	−2.5	−4.8			
	4K2m (224)	−17.5 (OC)				
	4K2m (225)	−0.6	−5.3	17,280 ± 100	carbonate	Beta-53653
	4K2m (230)	−1.4	−4.9			
	4K2m (255)	−3.3	−5.1			
	4K3 (280)	−2.7	−5.2			
3 (90-2)	E (0–10)	−6.6	−4.8			
	Bk (10–80)	−6	−4.7			
	2Bk (170–215)	−4.7	−5.1			
	3Bk (245–265)	−4.9	−6			
	4Btk (315–345)	−2.3	−6.7	13,010 ± 90	carbonate	Beta-75501
	4Btk (315–345)	−2.7	−5.3			
4 (90-3)	C (0–5)	−4.8	−5.4			
	Bk (5–90)	−5.1	−4.9			
	2Ak (90–140)	−3.8	−5			
	2Btk (140–200)	−2.7	−4.8			
	3Btk (200–225)	−3.08	−6	6,720 ± 80	carbonate	Beta-75503
	3Btk (200–225)	−3.06	−4.97			
	3K2 (225–235)	−0.8	−5.1			
5 (90-4)	A (0–15)	−4.26	−1.97			
	Btk1 (15–80)	−2.45	−4.67			
	2Btk2 (80–200)	−5.89	−6.23			
	2Btk2 (80–200)	−5.81	−6.47			

Table 2 (continued)

Site (name)	Horizon (cm)	$\delta^{13}C$ (PDB)	$\delta^{18}O$ (PDB)	^{14}C age years B.P.	Dated material	Lab. No.
	2K2 (200–240)	−1.49	−5.66			
	2K2 (200–240)	−1.4	−5.8	17,950 ± 90	carbonate	Beta-80871
	2K3 (240–275)	−2.41	−5.61			
6 (90-5)	A (0–15)	−5.05	−5.75			
	Css (15–215)	−5.07	−5.42			
	2Btk (215–270)	−4.99	−5.4			
	2Btk (215–270)	−5.8	−7.5	8,970 ± 210	carbonate	Beta-80872
7 (JI Lam.)	K2m (40.3)	−1.4	−4.5	9,680 ± 70	carbonate	Beta-47695
	K2m (40.8)	−1.7	−5.7	15,900 ± 90	carbonate	Beta-47696
	K2m (41.2)	−1.5	−5.4	30,630 ± 580	carbonate	Beta-47697
8 (91-1)	C (+20)	−6.9	−5.4			
	Bk (20)	−5.8	−4.6			
	Bk (25)	−5.8	−4.7			
	C′ (140)	−7	−5.7			
	C′ (140)	−22(OC)				
	2Bk (180)	−2.9	−5			
	2Bk (180)	−16.9 (OC)				
	2Bk (180)	−2.9	−5.2			
	2Bk (180)	−2.6	−4.9	9,070 ± 70	carbonate	Beta-51877
	3Btk1 (220)	−2.2	−5.6			
	3Btk1 (220)	−15.7 (OC)				
	3Btk1 (220)	−1.6	−5.4			
	3K2t (240)	−1.4	−5.5	23,070 ± 190	carbonate	Beta-53654
9 (91-4)	A (0–18)	−5.2	−6.36			
	Ak (18–30)	−6.77	−6.42			
	Btk (30–90)	−3.18	−4.27			
	Cgk (90–140)	−6.44	−5.62			

	Cgk (90–140)	−6.45	−5.56			
	2Btgk (140–190)	−4.83	−5.9			
	2K21g (190–225)	−1.75	−5.15			
	2K21g (190–250)	−1.7	−5.5	13,380 ± 90	carbonate	Beta-80873
	2K22g (250–330)	−2	−5.38			
10 (OCL)	C1 (15)	−4.2	−5			
	C2 (30)	−4.7	−4.5			
	E (45)	−5.1	−4.9			
	Btk (55)	−3.1	−5			
	Bk1 (70)	−3	−5.9	8,220 ± 120	carbonate	Beta-55376
	Bk2 (100)	−3.7	−5			
	Bk3 (120)	−3.4	−5.6			
	Bk4 (140)	−3.4	−6			
	E′ (153)	−3.7	−5.7			
	B′tk (183)	−3.9	−4.9			
	2Btk1 (218)	−3.1	−4.7			
	2Btk2 (238)	−3.3	−6.6	12,260 ± 130	carbonate	Beta-55377
	2K3t (298)	−1.7	−5.4	26,780 ± 310	carbonate	Beta-55378
11 (T. Well)	Bk (30)	−4.3	−6.2	8,590 ± 140	carbonate	Beta-55379
	2Bk (75)	−4.1	−5.7	5,380 ± 60	carbonate	Beta-55380
12 (ATr)	Ck (85)	−2.1	−4.4	9,930 ± 70	carbonate	Beta-53651
13 (Tr 7b)	Ck (52)	−3	−4.8	11,320 ± 70	carbonate	Beta-54925
	2Btk2 (75)	−4.2	−5.3	7,080 ± 100	carbonate	Beta-51883
	2K2m (97)	−3.8	−7	18,460 ± 100	carbonate	Beta-51882

Table 2 (continued)

Site (name)	Horizon (cm)	$\delta^{13}C$ (PDB)	$\delta^{18}O$ (PDB)	^{14}C age years B.P.	Dated material	Lab. No.
14 (1×1 Tr)	2Bk (120)	−3.8	−2.6	3,070±200	carbonate	Beta-54924
	3Bk (170)	−3.2	−0.6	4,170±200	carbonate	Beta-54923
	4K2m (228)	−4.2	−6.2	21,900±190	carbonate	Beta-54922
15 (Tr 5)	K2m (120.5)	−4.6	−4.9	7,700±60	carbonate	Beta-51878
	K2m (121)	−5	−7.6	15,910±90	carbonate	Beta-51879
	K2m (121.5)	−4.2	−7.4	23,440±200	carbonate	Beta-51880
	K2m (122)	−3.2	−6.7	26,870±260	carbonate	Beta-51881
16 (H. Mtn.)	A (2)	−6	−5.3			
	B (25)	−7.3	−5.4			
	Bk (80)	−7.3	−5.5			
	C (150)	−4.3	−5.6			
	2Btk (175)	−11.1	−7.6			
	2Btk (175)	−9.4	−9	10,790±70	carbonate	Beta-75505
	2Bk (240)	−2.6	−5.9			
	2C (290)	−0.9	−4.8			
	3Bk1 (333)	−2.9	−4.9			
	3Bk1 (333)	−1.1	−7.9	18,960±150	carbonate	Beta-75507
	3Bk2 (350)	−0.3	−4			
17 (T16)	Ck (95)	−2.7	−3.5	9,930±70	carbonate	Beta-53652
18 (SB1)	K2m (190)	−3.9	−6	26,650±600	carbonate	Beta-53191
19 (SB2)	2K2 (200)	−0.9	−5.1	14,360±120	carbonate	Beta-53190
20 (SB3)	2K2 (300)	−3.7	−7.1	23,140±170	carbonate	Beta-53192
21 (BPR)	Bishop’s Cap Study			Van Devender (1990)		
22 (HPR)	Hueco Mountain Study			Van Devender (1990)		
23 (F. Mtn.)	K2m1 (10)	−3	−5.2			

	K2m2 (50)	−6.5	−5			
	K2m3 (90)	−9.7	−6.6			
	2Btk (140)	−7.2	−7.2			
	2Bk (265)	−4.39	−6.85			
	3K2m (400)	−4.9	−6.8			
	3Btk (425)	−4.9	−7.1			
	3Bk (445)	−5.4	−6.8			
24 (FP)	Desert Project Pollen			Freeman (1972)		
25 (FB791332)	A (55)	−26.5		980 ± 70	charred	Beta-71680
	2Btk1 (150)	−4.4		4,570 ± 60	carbonate	Beta-71681
	2Btk2 (180)	−4.3		4,940 ± 80	carbonate	Beta-71682
26 (FB1)	Ck (50)	−3.6		8,920 ± 60	carbonate	Beta-71684
27 (FB7)	Ck (200)	−3.5		9,910 ± 70	carbonate	Beta-71683
28 (Blair)	White Sands Study			Blair et al. (1990)		
29 (Fil. Pass)	Btk (90)	−24.5 (OC)		3,930 ± 80	charcoal	Beta-63501
	2C (160)			4,060 ± 70	charred	Beta-65204
	2C (180)			4,100 ± 90	charred	Beta-65205
	3C (245)			4,100 ± 70	charred	Beta-65206

Depths represent average of 10 cm sampling zones, except where sampling ranges are indicated and laminae samples, which are shown in Figs. 2 and 5. Isotopic values are of carbonate except where labeled (OC) for organic carbon.

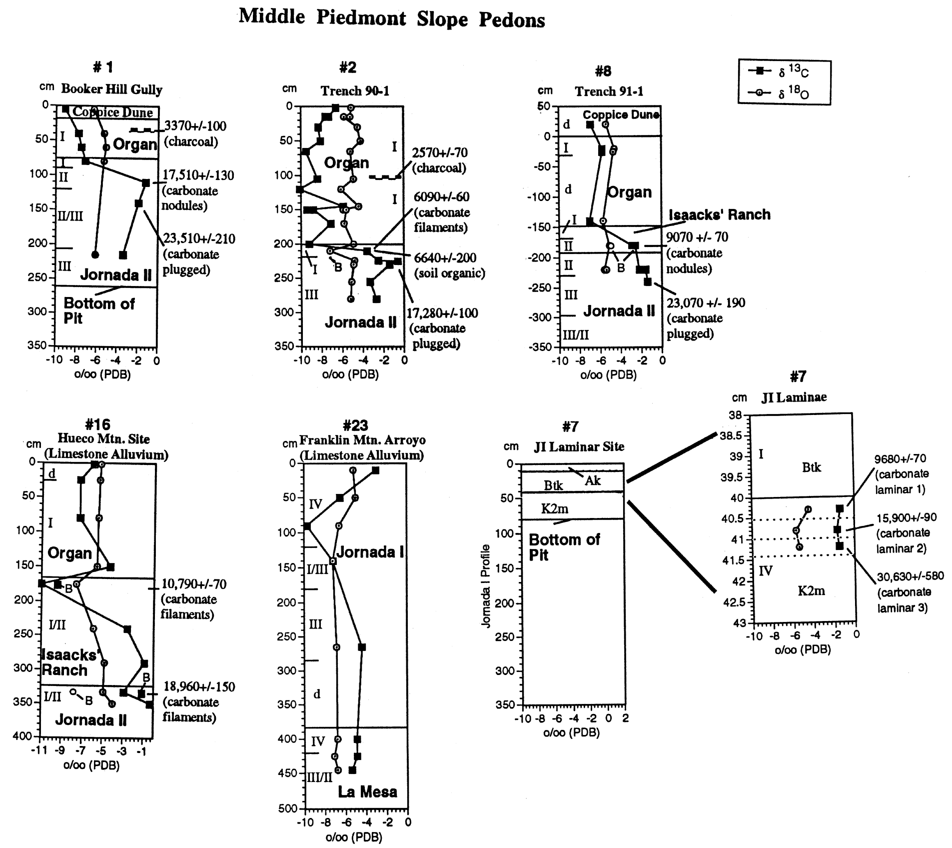

Fig. 3. Stable isotopic values and corresponding depths, morphogenetic carbonate stages (*I* through *IV*), and allostratigraphic units of the middle piedmont slope. Disseminated carbonates indicated with *d*. Radiocarbon ages are in years B.P. Material dated is in parentheses. Carbonate 'plugged' refers to k-fabric in stage III K horizon (Gile et al., 1965). In sites 8 and 16, subsample splits were sent to Beta Analytic, Inc., indicated with a '*B*'. Sites 7 and 23 are relict paleosols not buried by Organ sediments. Coppice dunes in the region generally began forming during the last 150 years (Gile, 1966).

the lower piedmont slope–playa depressions, the magnitude of the $\delta^{13}C$ shifts across Organ discontinuities are dampened (Fig. 4). In the eolian basin floor, $\delta^{13}C$ shifts are difficult to ascertain because the isotopic record is less complete (Fig. 5). However, little $\delta^{13}C$ change occurs at site 14 for the upper stage IV laminar layer and overlying stage I filaments (Fig. 5).

$\delta^{18}O$ shifts are minor on the middle piedmont across Organ discontinuities (Fig. 3). Similarly, $\delta^{18}O$ values in the lower piedmont slope–playa depressions remain relatively constant across the $\delta^{13}C$ shifts, with the exception of site 5 that contains an enriched surface sample (Fig. 4). The basin floor, in contrast, contains greater $\delta^{18}O$ shifts, especially site 14 (Fig. 5).

Fig. 6 plots the relationship between of $\delta^{13}C$ and $\delta^{18}O$ data and their variability for the three landform categories. The middle piedmont slope has the

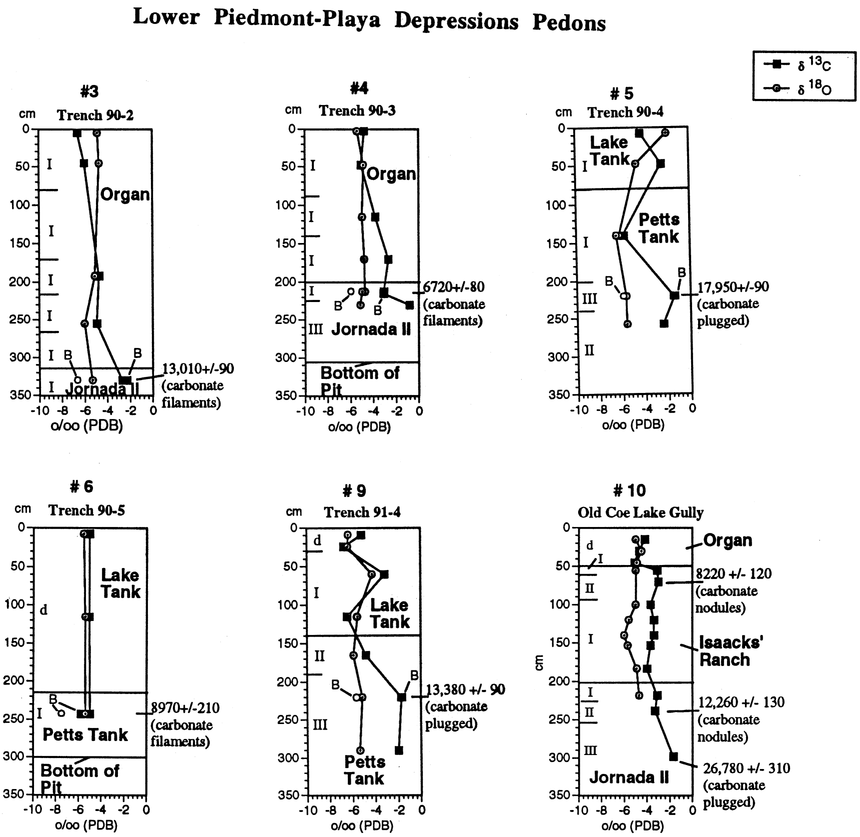

Fig. 4. Stable isotopic values and corresponding depths, morphogenetic carbonate stages (*I* through *IV*), and allostratigraphic units of the lower piedmont slope and tectonic playa depressions. Disseminated carbonates indicated with *d*. Radiocarbon ages are in years B.P. Carbonate 'plugged' refers to k-fabric in stage III K horizon (Gile et al., 1965). Material dated is in parentheses. Several subsample splits were sent to Beta Analytic, Inc. which are indicated with a *B*.

highest $\delta^{13}C$ variability, with a mean $\delta^{13}C$ value of -4.5‰ and a standard deviation (s.d.) of 2.8‰, followed by the lower piedmont slope–playa depressions (mean -3.9‰, s.d. 1.6‰), with least $\delta^{13}C$ variability in the basin floor (mean -3.6‰, s.d. 1.0‰). The variability of $\delta^{18}O$ is greatest in the basin floor (mean -5.4‰, s.d. 1.8‰), followed by the middle piedmont (mean -5.7‰, s.d. 1.0), with least $\delta^{18}O$ variability in the lower piedmont slope–playa depressions (mean -5.4‰, s.d. 0.8‰).

Most pedons occur in igneous alluvium or quartzose eolian material. Two pedons, however, occur in limestone alluvium: nos. 16 and 23. Pedon 16 is located on the middle piedmont slope of the Hueco Mountains (Fig. 1). Its isotopic shift across the Organ discontinuity is similar to pedons on the igneous piedmont slope (Fig. 3). The other limestone pedon, no. 23, contains the oldest

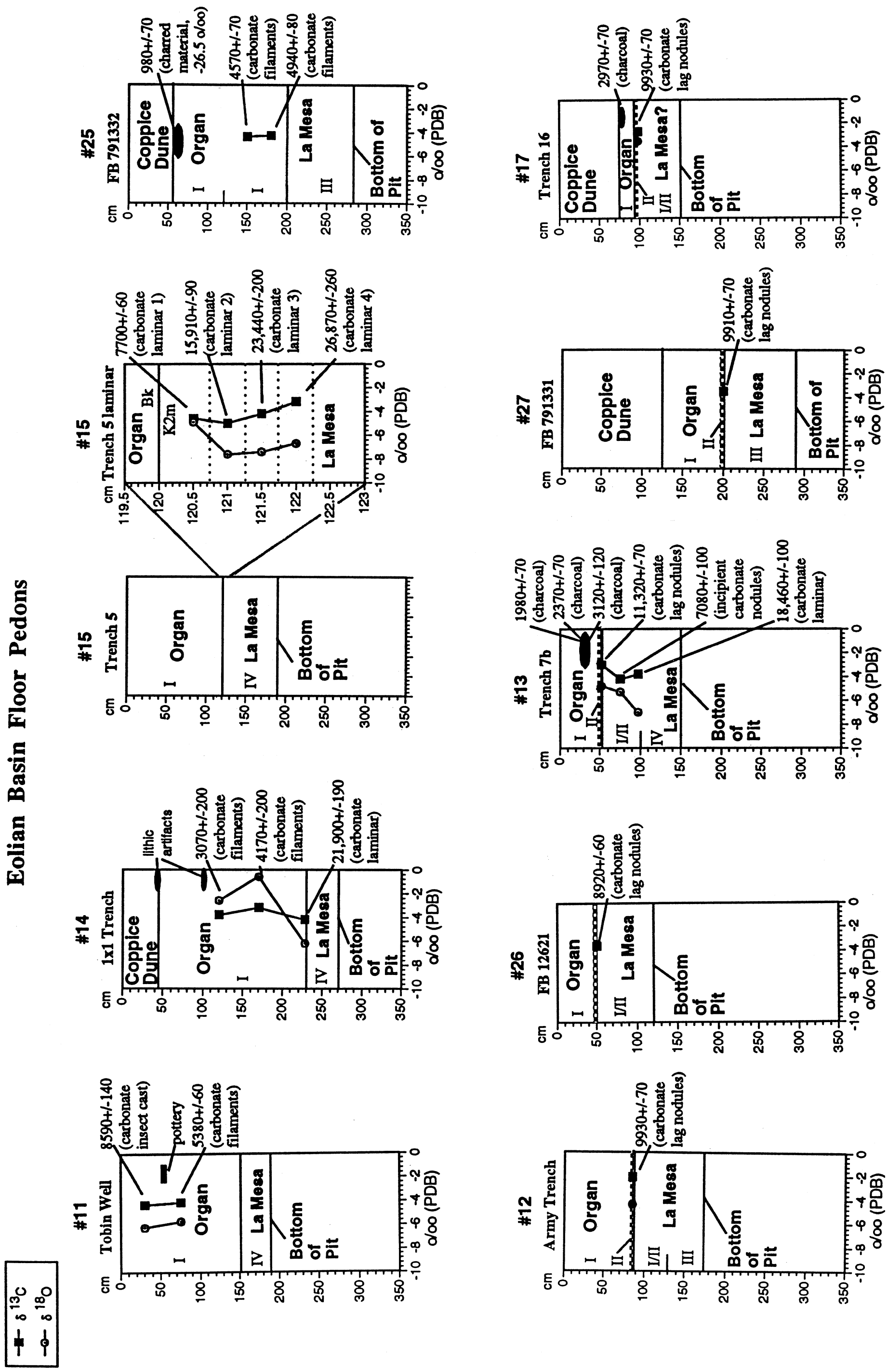
Eolian Basin Floor Pedons
δ13C
δ18O
#11
Tobin Well
8590+/-140 (carbonate insect cast)
pottery
5380+/-60 (carbonate filaments)
Organ
La Mesa
Bottom of Pit
#14
1x1 Trench
Coppice Dune
lithic artifacts
3070+/-200 (carbonate filaments)
4170+/-200 (carbonate filaments)
21,900+/-190 (carbonate laminar)
Organ
La Mesa
Bottom of Pit
#15
Trench 5
Organ
La Mesa
Bottom of Pit
#15
Trench 5 laminar
7700+/-60 (carbonate laminar 1)
15,910+/-90 (carbonate laminar 2)
23,440+/-200 (carbonate laminar 3)
26,870+/-260 (carbonate laminar 4)
Organ
Bk
K2m
La Mesa
#25
FB 791332
980+/-70 (charred material, -26.5 o/oo)
4570+/-70 (carbonate filaments)
4940+/-80 (carbonate filaments)
Coppice Dune
Organ
La Mesa
Bottom of Pit
#12
Army Trench
9930+/-70 (carbonate lag nodules)
Organ
La Mesa
Bottom of Pit
#26
FB 12621
8920+/-60 (carbonate lag nodules)
Organ
La Mesa
Bottom of Pit
#13
Trench 7b
1980+/-70 (charcoal)
2370+/-70 (charcoal)
3120+/-120 (charcoal)
11,320+/-70 (carbonate lag nodules)
7080+/-100 (incipient carbonate nodules)
18,460+/-100 (carbonate laminar)
Organ
La Mesa
Bottom of Pit
#27
FB 791331
9910+/-70 (carbonate lag nodules)
Coppice Dune
Organ
La Mesa
Bottom of Pit
#17
Trench 16
2970+/-70 (charcoal)
9930+/-70 (carbonate lag nodules)
Coppice Dune
Organ
La Mesa?
Bottom of Pit
cm
o/oo (PDB)

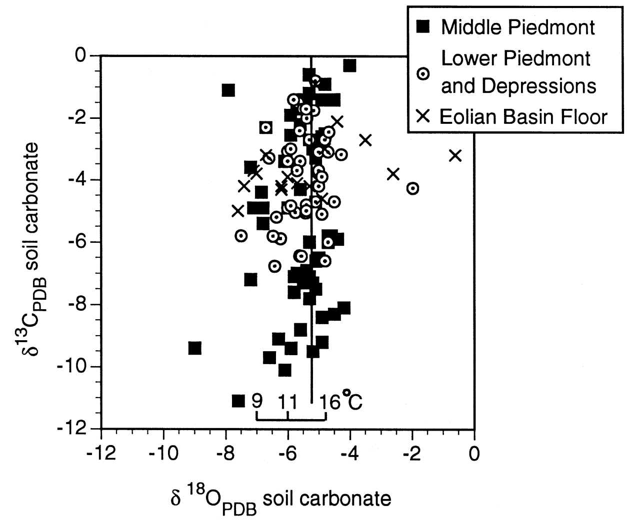

Fig. 6. Relationship between $\delta^{13}C$ and $\delta^{18}O$ for three landform categories. Temperature scale relates theoretical mean annual air temperatures to $\delta^{18}O$ values based on model by Hays and Grossman (1991). Vertical line represents mean annual air temperature of 15°C in study region of southern New Mexico and west Texas.

strata of this study, possibly dating from middle to early Pleistocene or older (Table 1). This site also contains a shift toward depleted $\delta^{13}C$ values. However, the shift is older and uniquely occurs within a stage IV petrocalcic horizon (Fig. 3).

4.2. Fossil pollen

Pollen and isotope data from the same depths are compared in Fig. 7 for three pedons: no. 1 (Booker Hill Gully), no. 2 (90-1), and no. 10 (Old Coe Lake Gully). Two pedons (1 and 2) occur on the middle piedmont slope of the Organ Mountains (Fig. 7A,B). The third, pedon (10), occurs in the lower piedmont–playa depression (Fig. 7C). The Cheno-Am taxon includes all Chenopodiaceae (except *Sarcobatus*, greasewood) and *Amaranthus* (in the Amaranthaceae plant family). The two middle piedmont slope pedons display increased Cheno-Am pollen at the Organ discontinuities. In contrast, the depression site displays a less discernable shift at that boundary (Fig. 7C). Accompanying the Cheno-Am shift in the middle piedmont slope pedons, is a decline in grass pollen. This is more pronounced for site 1 than for site 2 (Fig. 7A,B).

Fig. 5. Stable isotopic values and corresponding depths, morphogenetic carbonate stages, and allostratigraphic units of the eolian basin floor. Radiocarbon ages are in years B.P. Material dated is in parentheses. ^{14}C ages of charcoal at sites 13 and 17 from Jeff Leach (pers. commun., 1994. Dates on file with Fort Bliss Environmental Management Office).

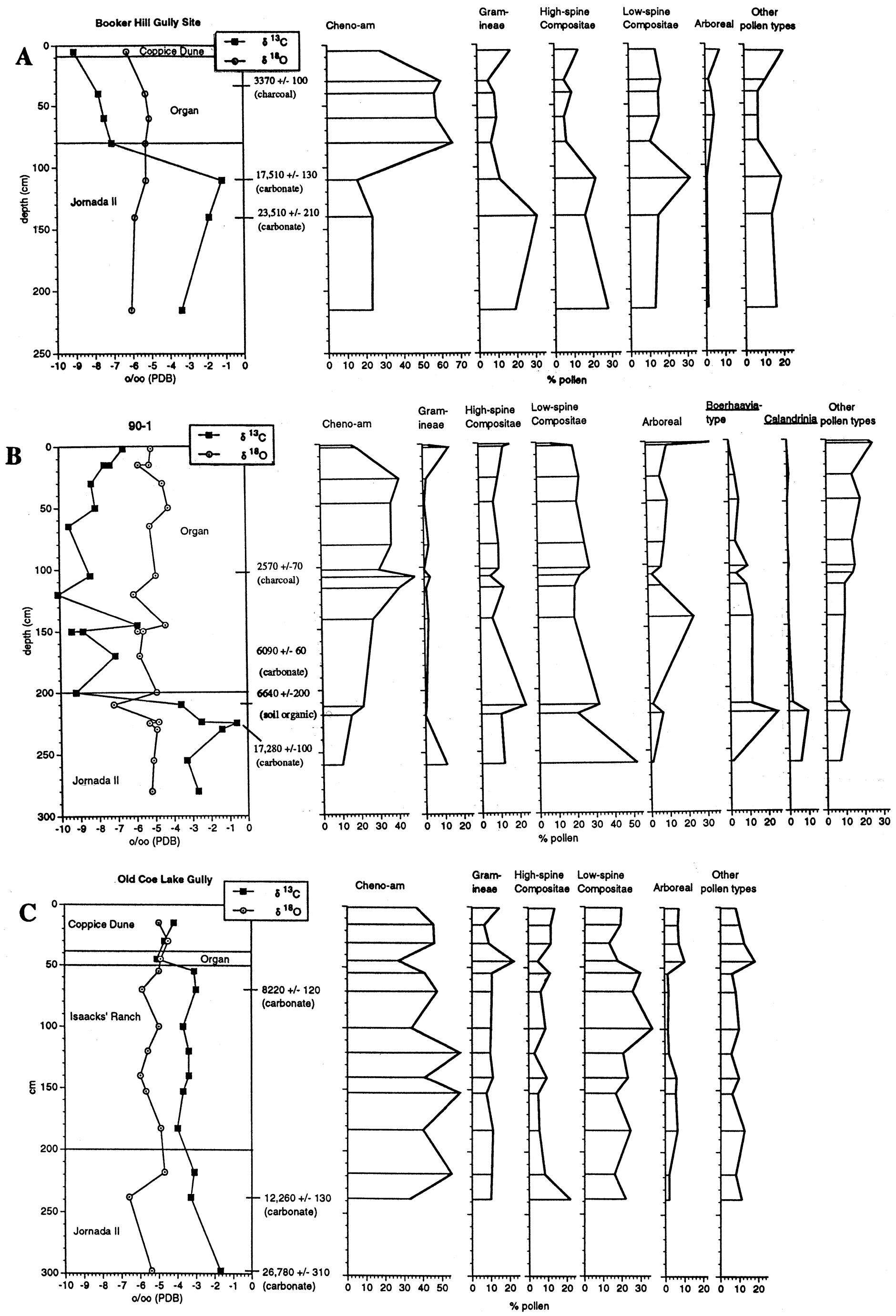

Fig. 7. Stable isotope and pollen comparison for three sites: 1 (Booker Hill Gully); 2 (90-1); and 10 (Old Coe Lake).

A comparison of pollen and isotopes reveals some similar trends (Fig. 7). The Booker Hill Gully site shows a major increase in Cheno-Am pollen and decline in grass pollen corresponding to a 6‰ shift toward lower $\delta^{13}C$ values (Fig. 7A). The other middle piedmont site, 90-1, shows an increase in Cheno-Am pollen in Organ alluvium, also corresponding to a shift in $\delta^{13}C$ values (Fig. 7B). Although the trends are the same, the 90-1 site has a less abrupt Cheno-Am increase and less grass pollen than Booker Hill. The third pollen site, Old Coe Lake, shows minor pollen changes. Correspondingly, the carbon isotope values also show subtle change in $\delta^{13}C$ values from -3 to -5.5‰ (Fig. 7C).

5. Discussion

With the possible exception of site 16 (Fig. 3), soils of the middle piedmont slopes and lower piedmont slope–playa depressions do not appear to have been significantly truncated when buried. This observation is based on comparison to neighboring unburied soil profiles. However, this is not the case for several profiles in the basin floor. These eolian profiles contain carbonate nodules and Rio Grande pebbles concentrated into layers beneath the Organ unit (Fig. 5). As noted by Blair et al. (1990), these layers appear to be erosional lag layers.

5.1. Age of Organ alluvium

The most prominent $\delta^{13}C$ shifts occur at discontinuities underlying Organ alluvium. Therefore, the timing of Organ alluviation is important. Organ deposits were first described by Ruhe (1964, 1967), who recognized their young age based on their geomorphic position and weak profile development. Gile (1975) estimated that the deposition of Organ sediments began about 7500 years B.P. based on a sequence of ^{14}C-dated charcoal deposits in the Desert Project (Fig. 1). The oldest charcoal deposit of 6400 ± 110 years B.P. was in the lower part, but not the base, of Organ sediments overlying a Jornada II geomorphic surface. He thus postulated that Organ alluviation may have started with Antevs' altithermal (Antevs, 1955). Later, the age estimate was changed from 7500 to 7000 years B.P. (Gile et al., 1981).

Other evidence for Organ's age comes from its correlative mapping unit in the adjoining Rio Grande river system: the Fillmore unit (Gile et al., 1981). Like Organ, Fillmore alluvium is mapped based on its lowest geomorphic position, which is graded near the level of modern arroyos, its stage I carbonate filaments, and its weak or absent argillic horizon. Fillmore alluvium contains a sequence of ^{14}C-dated charcoal deposits that span a period from 7340 ± 285 to 2620 ± 200 years B.P. (Fig. 8). Underlying the Fillmore unit is the Leasburg unit, which is correlative to the Bolson Isaacks' Ranch unit. The Leasburg unit has a ^{14}C on charcoal of 9360 ± 150 years B.P. (Fig. 8).

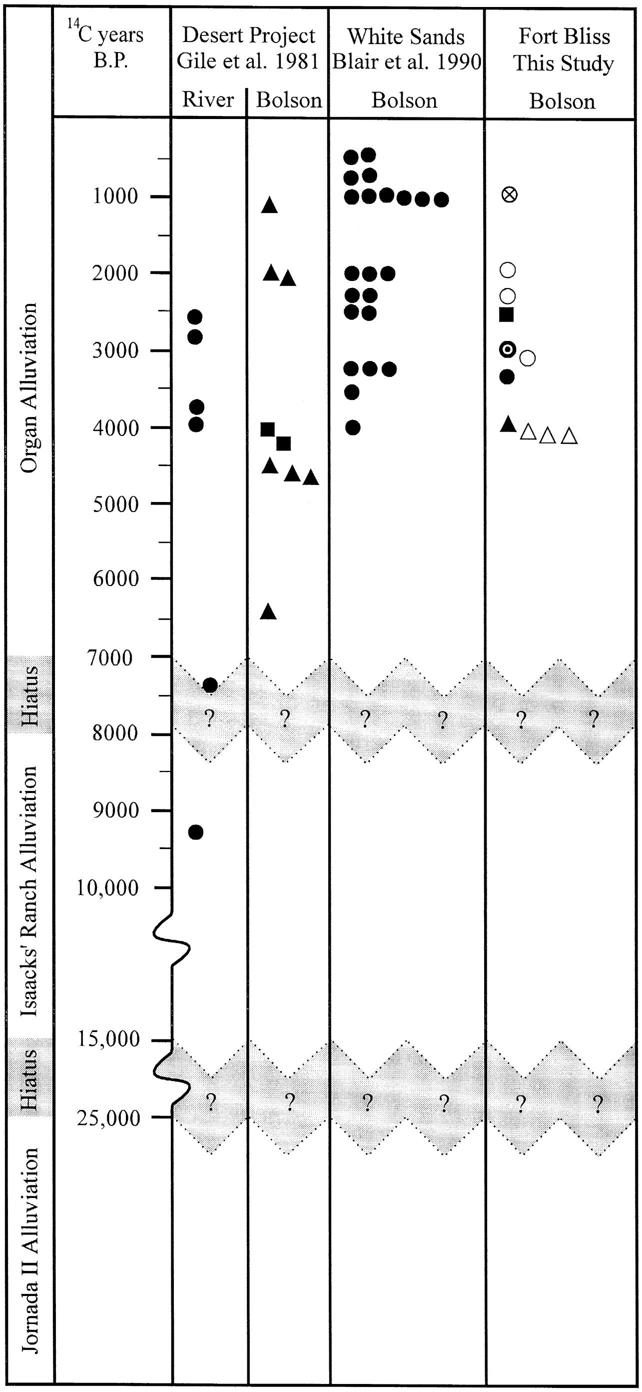

^{14}C years B.P.
Desert Project Gile et al. 1981
River
Bolson
White Sands Blair et al. 1990
Bolson
Fort Bliss This Study
Bolson
1000
2000
3000
4000
5000
6000
7000
8000
9000
10,000
15,000
25,000
Organ Alluviation
Hiatus
Isaacks' Ranch Alluviation
Hiatus
Jornada II Alluviation
?

Subsequent to the Desert Project, several ^{14}C ages of charcoal have be collected from Organ sediments on Fort Bliss and White Sands Missile Range. Blair et al. (1990) report 22 radiocarbon dates from their study area on White Sands (Figs. 1 and 8). On Fort Bliss, eleven ^{14}C ages have been measured (Fig. 8). Much of the charcoal found in the Organ unit are the remains of camp fires or other anthropogenic activity. By plotting several hundred radiocarbon-dated archaeological features in the Fort Bliss area, Mauldin (1995) found that most features are between 5000 and 200 years B.P., with the greatest number of features dating to about 1000 years B.P.

5.2. ^{14}C ages of pedogenic carbonates

Pedogenic carbonate accumulates in a time-transgressive manner. Therefore, the ^{14}C age of a pedogenic carbonate sample, as well as its stable isotopic composition, represent an average for that sample (Wang et al., 1996). Even a small sample from a stage IV petrocalcic horizon, for example, will be composed of many thousands of calcite crystals (e.g., Monger et al., 1991b). In contrast, stage I filaments contain fewer calcite crystals and, when radiocarbon-dated represent a much shorter interval of time.

In this study, all four carbonate morphogenetic stages were radiocarbon-dated. The ^{14}C ages of filaments from the Organ unit fell within Organ's estimated age of 7000 to 100 years B.P. (Gile et al., 1981). These filament ages were 5380 ± 60 at site 11, 3070 ± 200 and 4170 ± 200 at site 14, and 4570 ± 70 and 4940 ± 80 years B.P. at site 25 (Fig. 5). Five soils buried by Organ sediments also contain carbonate filaments in their upper sola. The ^{14}C ages of these filaments are 6090 ± 60 at site 2, $10,790 \pm 70$ at site 16, $13,010 \pm 90$ at site 3, 6720 ± 80 at site 4, and 8970 ± 210 years B.P. at site 6 (Figs. 3 and 4). Stage II, III, and IV carbonates in paleosols beneath Organ sediments all had ^{14}C ages greater than 7000 years B.P. (Figs. 3–5).

With the exception of two pedons, all carbonate ^{14}C ages are progressively older at progressively greater depths. One exception occurs at site 11 where a calcareous insect cast had a ^{14}C age of 8590 ± 140 (Figs. 5 and 9). This site occurred in a deflated region where soil profiles were truncated and petrocalcic fragments littered the land surface. A subsample of the radiocarbon-dated insect cast was examined with scanning electron microscopy (SEM). All grains in this

Fig. 8. Charcoal ^{14}C age-control for Organ alluviation in Desert Project, White Sands, and Fort Bliss (located in Fig. 1). 'River' column refers to charcoal in Fillmore alluvium (correlative to Organ) and Leasburg alluvium (correlative to Isaacks' Ranch). Symbols in Fort Bliss column represent the following sites located in Fig. 1 and Table 2: circle containing $\times$ = site 25; open circle = site 13; solid square = site 2; circle with dot = site 17; solid circle = site 1; solid triangle = site 29; open triangle = charred material at site 29. Stratigraphic context of Fort Bliss charcoal samples are illustrated in Figs. 3-5.

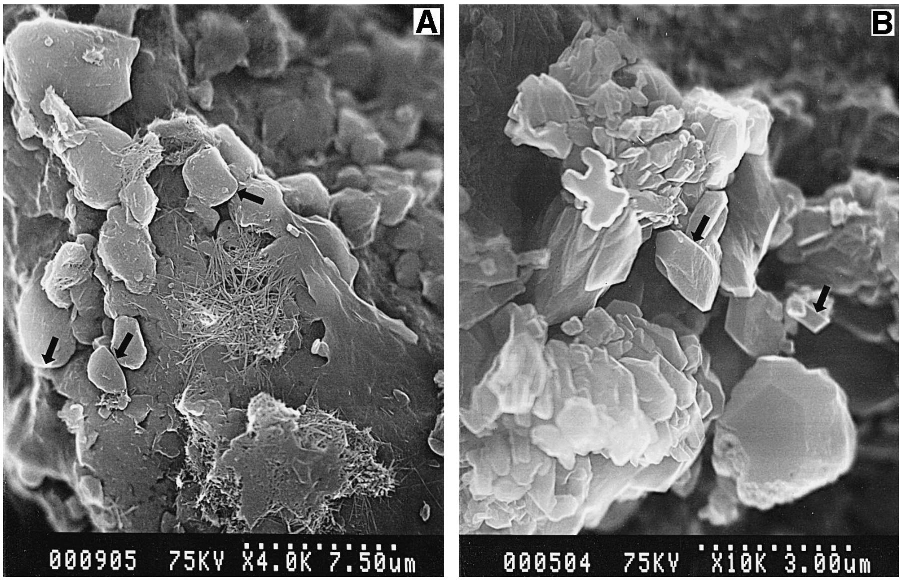

Fig. 9. Scanning electron micrographs of ^{14}C-dated carbonate samples. (A) Carbonate material in insect cast at site 11 with ^{14}C age of 8590 ± 140 years B.P. (Fig. 5). This date appears too old because it overlies pottery artifacts less than about 1600 years B.P. (Carmichael, 1986). Note rounded nature of all grains (arrows), suggesting transport or dissolution. (B) Carbonate material in uppermost laminar layer at site 15 with ^{14}C age of 7700 ± 60 years B.P. (Fig. 5). This date is in the correct superposition order, being the youngest date overlying a series of progressively older laminae. Note euhedral nature of grains including rhombohedral crystals (arrows), suggesting in situ precipitation.

subsample are rounded, suggesting eolian transport or dissolution (Fig. 9A). For comparison, a sample in the correct superposition (i.e., younger on top) was also observed with SEM. This sample was the uppermost laminar sample from site 15 (Fig. 5). In contrast to the rounded grains from site 11, grains in this sample were rhombohedral-shaped crystals, suggesting in situ precipitation (Fig. 9B).

The second exception to the pattern of progressively older carbonate at progressively greater depths occurred at another eolian basin floor site, no. 13 (Fig. 5). At this site, stage II 'lag' nodules, representing a paleodeflational surface, are underlain by younger incipient nodules, which appear to be forming in situ based on their diffuse boundaries with surrounding soil matrix. This stratigraphically reversed relationship may represent the destruction of a former soil profile by deflation, whereby the carbonate nodules collapsed vertically, followed by the formation of incipient nodules until burial by Organ sediments when the depth of wetting and carbonate deposition shifted upward.

Otherwise, pedons had progressively older carbonate ^{14}C ages with depth, which is a pattern predicted by the production–diffusion model of Amundson et al. (1994) and Wang et al. (1994). This model emphasizes that soil CO_2, the master variable controlling ^{14}C content in pedogenic carbonate, is derived from two sources: root respiration and microbial decomposition (Wang et al., 1994). Although the ^{14}C content of CO_2 from root respiration is ca. 0 radiocarbon years, the CO_2 from microbial decomposition can have radiocarbon ages that are several thousand years B.P., making carbonate samples appear older than they really are.

Application of the ^{14}C model of Amundson et al. (1994) and Wang et al. (1994, 1996) to ^{14}C ages in this study is complicated for two reasons. First, their model applies to non-aggrading, relict soils and assumes carbonate accumulation since soil formation began. Many soils in this study, however, are buried and out of the zone of modern carbonate deposition, and thus the pedogenic carbonate is not cumulative over the life span of the soil. Second, the amount and type of soil organic matter and respiration rates may have changed significantly over the life

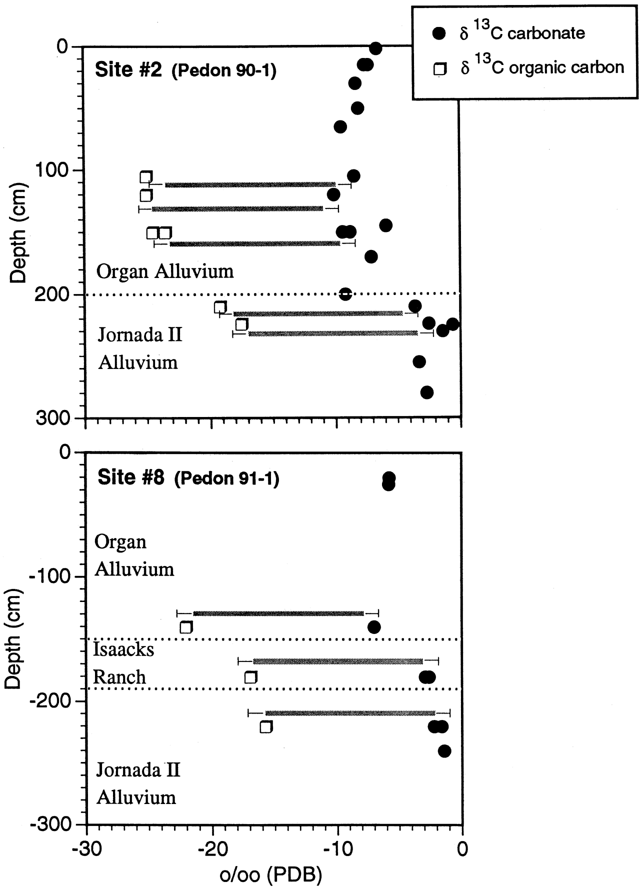

Fig. 10. Illustration of enrichment of carbonate with respect to associated organic matter for sites 2 (90-1) and 8 (91-1). Carbonate and organic matter are expected to differ by 14‰ to 16‰ if cogenetic (Cerling et al., 1989). Thick portion of horizon bar represents 14‰, total bar length represents 16‰.

span of the soils. Currently, soil organic carbon content is much less than 0.5% in most soils, especially the coarse, desert scrub soils that can have A horizons with values as low as 0.19% (Gile and Grossman, 1979). During pluvial periods of the Late Pleistocene, however, vegetation density, soil organic matter, and respiration rates may have been significantly higher.

Another important process that could affect ^{14}C content in pedogenic carbonates, especially at shallow depths, is dissolution and reprecipitation (Pendall et al., 1994). As evidence of dissolution–reprecipitation, Pendall et al. (1994) reported enrichment of $\delta^{13}C$ and $\delta^{18}O$ values toward the soil surface. Most of the soils in our study, however, do not have distinct $\delta^{13}C$ and $\delta^{18}O$ enrichment trends towards the land surface (Figs. 3 and 4). In fact, several of the buried soils show depleted $\delta^{13}C$ values toward former land surfaces (i.e., sites 1, 2, 8, 16, and 4). A comparison of organic and carbonate $\delta^{13}C$ values at two sites (2 and 8) reveals that carbonates are enriched 14 to 16‰ with respect to associated

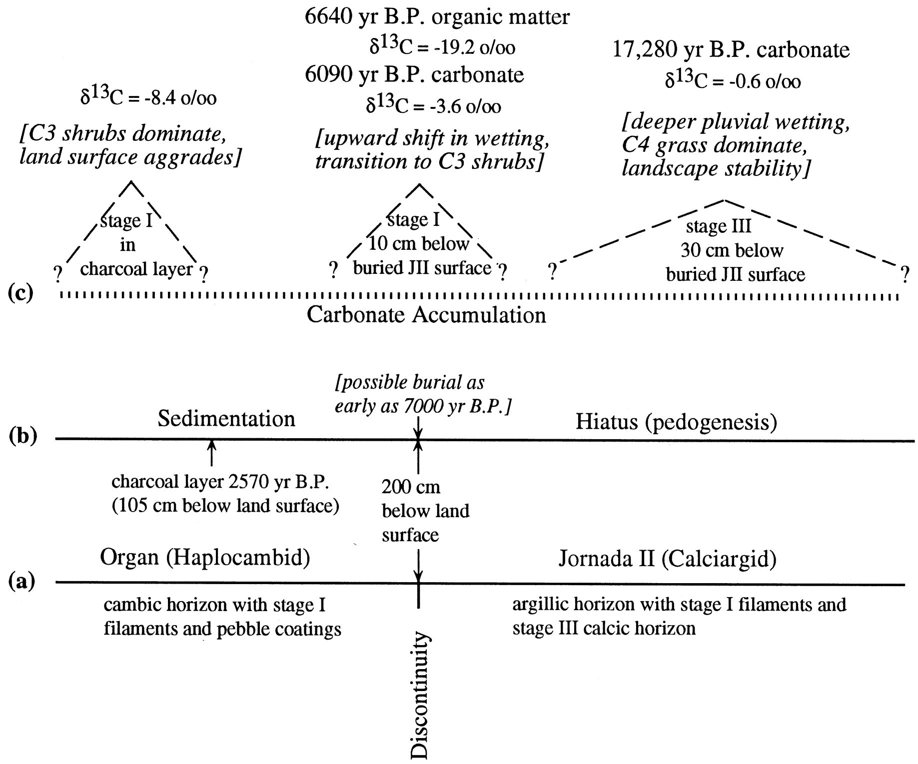

Fig. 11. Conceptual model relating carbonate ^{14}C ages to landscape evolution. Line (*a*) illustrates soil morphology and classification. Line (*b*) is interpretation of sedimentation history based on Line (a) and charcoal at 105 cm. Line (*c*) illustrates hypothetical time spans (dashed lines) of carbonate and organic matter accumulation based on assumption that carbonate deposition zone lifted and travelled upward with aggrading land surface. Paleoenvironmental interpretations are given as italicized text in brackets.

organic matter (Fig. 10); a range suggesting that organic matter and carbonate are cogenetic (Cerling et al., 1989). This pattern across former land surfaces suggests that the isotopic values were not controlled by dissolution–reprecipitation.

Instead of dissolution–reprecipitation, aggradation may have played a larger role in controlling ^{14}C and ^{13}C patterns. As an example, an aggradation scenario is illustrated in Fig. 11 using site 2 (pedon 90-1). Line (a) represents the soil morphology and classification. Line (b) represents a possible sedimentation history where argillic and calcic horizons indicate substantial pedogenesis during a hiatus before burial by Organ. Charcoal at 105 cm in the Organ unit indicates 1 m of sedimentation before and 1 m after about 2570 years B.P. Line (c) represents progressive accumulation of pedogenic carbonate crystals. The ^{14}C age of the stage III calcic horizon at about 30 cm below the buried Jornada II surface represents carbonate accumulation during an unknown interval before and after 17,280 years B.P. Stage I filaments in the argillic horizon of the Jornada II soil span a much shorter accumulation interval. Like the ^{14}C age of the underlying stage III calcic, the ^{14}C ages of carbonate filaments (6090 years B.P.) and organic matter (6640 years B.P.) probably represent average ages whose exact beginning and ending are uncertain.

With commencement of sedimentation, however, carbonate deposition was presumably pulled upward, out of the Jornada II soil, and traveled in a subsoil zone of about 15 to 45 cm beneath the aggrading land surface. Similarly, the zone of organic matter deposition would have lifted with aggradation. The ^{14}C age of charcoal at 105 cm indicates that the charcoal layer was deposited after 2570 years B.P. As aggradation continued, the charcoal layer would have been buried progressively deeper, causing the carbonate deposition zone to migrate through the charcoal sediments, and therein deposit stage I filaments and pebble coatings.

5.3. $\delta^{13}C$ values as paleovegetation indicators

In addition to dissolution–reprecipitation of carbonates described by Pendall et al. (1994), other factors can complicate the use of pedogenic carbonates as paleovegetation indicators. First, if plants are sparse and plant-respired CO_2 is low, atmospheric CO_2 (having a $\delta^{13}C$ average of about -6 to -8‰) can diffuse into the upper portion of the soil and enrich the carbonates (Cerling, 1984; Quade et al., 1989a; Wang et al., 1996). Second, if fossil organic matter remains in the soil, CO_2 from microbial decomposition could affect carbonate signatures (Wang et al., 1994). Third, desert succulents, such as cacti, are often admixed with both the C_4 grassland communities and C_3 shrubland communities. Succulents use the CAM photosynthetic pathway, producing isotopic values intermediate between C_4 and C_3 plants (Ehleringer, 1989). Fourth, *Atriplex* species, most notably fourwing saltbush, make up variable proportions of an otherwise C_3-dominated shrubland. Fifth, if limestone detritus is not removed before acid treatment to extract CO_2, it may alter the isotopic signal (Rabenhorst et al., 1984; Cerling and Quade, 1993).

In light of these factors, we see two plausible hypotheses that may explain the Organ-related isotopic shifts. The first hypothesis attributes the $\delta^{13}C$ shift to a change in respiration rates. The second hypothesis attributes the $\delta^{13}C$ shift to a change from C_4-dominated to C_3-dominated vegetation. If we take high respiration rates to indicate high plant density, and high plant density to indicate grasslands versus low plant density to indicate shrublands, the first hypothesis appears to contradict erosion–sedimentation evidence. This is because Jornada II soils have well-developed profiles, suggesting landscape stability for an extended period of time. Enriched ^{13}C values of the Jornada II calcic horizons would suggest lower respiration rates (or lower plant densities), rather than high plant density. Also, the ^{13}C shift toward lower values across the discontinuities would indicate increased respiration rates (or increased plant densities). If that were the case, the following question arises: 'would increased plant density correspond to erosion and the deposition of Organ alluvium?' Runoff experiments in southeastern Arizona reveal that overland flow, hence erosion, is greater in shrublands than in grasslands (Abrahams et al., 1995). Also, as predicted by the Universal Soil Loss Equation, decreased plant cover increases erosion.

In evaluating the second hypothesis, that attributes the $\delta^{13}C$ shift to a change from C_4-dominated to C_3-dominated vegetation, it is necessary to recognize that in many regions C_3 vegetation is adapted to cooler and more humid conditions, whereas C_4 vegetation is adapted to hotter and drier conditions (Cerling and Quade, 1993). However, in our study area the opposite situation occurs: C_3 plants are primarily desert shrubs that are adapted to hotter and drier conditions than the C_4 grasses which tend to occur at slightly higher elevations (Cole and Monger, 1994). If $\delta^{13}C$ values at site 1, for example (Fig. 3), record C_3 desert shrubs, the isotopic data corroborates the erosion data because bare ground and erosion accompany shrub conditions (Schlesinger et al., 1990). However, before the onset of Organ alluviation, when the Jornada II soil was at the land surface, C_4 grasses were dominant and would have curtailed erosion–sedimentation (Fig. 11). Therefore, it appears that the second hypothesis attributing the isotopic shift to a change from C_4 grasses to C_3 desert scrub vegetation was more likely than a change in respiration rates.

5.4. $\delta^{18}O$ values

Interpreting $\delta^{18}O$ values in soil carbonate can be complicated because ^{18}O content is controlled by both the isotopic signature of rain and any fractionation in the soil (Cerling, 1984; Cerling and Quade, 1993; Pendall et al., 1994; Liu et al., 1995; Amundson et al., 1996). The isotopic signature of rain, in turn, is influenced by several factors: (1) latitudinal location (isotopically lighter rain occurs poleward); (2) seasonality (winter rain is isotopically lighter and percolates deeper in the soil); (3) mountain ranges and distance from the coast (lighter rain at higher altitudes and greater distances from coast); (4) the amount of rain (rain becomes lighter as the amount of rain increases, this includes both monthly rainfall and individual rainfall events); (5) storm trajectories (source-area, including vapor from land, yields different $\delta^{18}O$ values); and (6) mean annual air temperature (as temperatures increase, $\delta^{18}O$ values increase) (Rozanski et al., 1993; Grootes, 1993). Fractionation of ^{18}O in soil also occurs because of (1) evapotranspiration, (2) elevated soil temperatures, and (3) reequilibration caused by dissolution and reprecipitation of carbonate (Cerling and Quade, 1993; Pendall et al., 1994), especially in hyper-arid soils (Amundson et al., 1996).

Despite these variables, Cerling and Quade (1993) reported a correlation ($r^2 = 0.84$) between $\delta^{18}O$ values in soil carbonate and meteoric water. In desert soils of southern Arizona, Liu et al. (1995) found that $\delta^{18}O$ varied seasonally in the upper 40 cm, with the highest $\delta^{18}O$ values occurring in the hot, dry seasons. Below 40 cm and deeper, the isotopic values became more closely related to the composition of the local average annual precipitation.

The $\delta^{18}O$ values in this study generally did not become progressively enriched near the land surface (Figs. 3 and 4). This trend is different than trends in the Great Basin, where $\delta^{18}O$ values are highest in surface samples, purportedly due to evaporative enrichment (Pendall et al., 1994) or a combination of evaporative enrichment and preferential infiltration where winter precipitation percolates more deeply (Quade et al., 1989a). More studies are needed to explain why neither $\delta^{18}O$ nor $\delta^{13}C$ values become enriched near the land surface. One possibility is that erosion may have removed the upper enriched portion of the profile, although erosional surfaces were not apparent except at site 16 and the sites containing lag nodules in the eolian basin floor.

Also, $\delta^{18}O$ values of soil carbonates in this study did not display pronounced shifts across Organ discontinuities, unlike the $\delta^{13}C$ shifts (Fig. 3). This discordant relationship led Cole and Monger (1994) to suggest that factors other than climate alone (most likely increased atmospheric CO_2), were responsible for the $\delta^{13}C$ shift. Liu et al. (1996) found a similar relationship of little change in $\delta^{18}O$ when $\delta^{13}C$ values changed about 4.5‰ in desert soils of Arizona. They interpreted the little change in $\delta^{18}O$ values to be the result of an increase in the carbonate–water fractionation factor with decreasing temperature that counteracted the decrease in the $\delta^{18}O$ of rainfall. This conclusion was arrived at because independent evidence indicated that glacial-period summer temperatures were probably much cooler, and that $\delta^{18}O$ of rainfall was lighter.

Although isotopic signatures of rainwater correlate with mean annual air temperatures (Dansgaard, 1964; Rozanski et al., 1993), and theoretical relationships have been developed that link carbonate $\delta^{18}O$ values to paleotemperatures (e.g., Hays and Grossman, 1991), changes in rainfall seasonality, storm trajectories, and differential enrichment in soil profiles may mask paleotemperature information. This appears be the case with the ^{18}O data in this study, which is suggested by the scatter in $\delta^{18}O$ values plotted in Fig. 6. If paleotemperatures alone accounted for the scatter, mean annual temperature changes in the late Quaternary would have been greater than 6°C, using the model of Hays and Grossman (1991). Amundson et al. (1996) concluded that $\delta^{18}O$ values in Wyoming soil carbonates were more useful for identifying past rainwater sources than for estimating paleotemperatures.

5.5. Implications for ecogeomorphic changes

5.5.1. Landscape stability–instability

Landscape stability is required for soil horizons to form. In contrast, periods of landscape instability (i.e., erosion and sedimentation) are times when deposition buries surface soils in aggrading environments. Therefore, stacked sequences of buried soils have been used as evidence for alternating periods of landscape stability and instability (Butler, 1959; Gile and Hawley, 1966; McDonald and Busacca, 1990; Bull, 1991). In the study region, erosion–sedimentation periods are thought to represent a decline in vegetation density, causing the production of fans, valley fills, and terraces (Hawley, 1975a). Within these aggradational environments, the stacked sequences of buried paleosols appear to correspond to glacial–interglacial periods (Hawley et al., 1976). As discussed earlier, the latest major period of landscape instability began about 7000 years B.P. as inferred from Organ and Fillmore alluviation (Gile et al., 1981).

The $\delta^{13}C$ shift toward more negative values across Organ discontinuities (Figs. 2 and 3) indicates a change from C_4-dominated flora to C_3-dominated flora. Because C_4 plants in the study area are grasses and C_3 plants are desert shrubs, this isotopic shift implies the decline of grasses and increase of shrubs. Based on observations of modern desert vegetation, this increase in desert shrubs would have increased bare ground and erosion upslope, resulting in Organ deposition downslope. In this model, the stable isotopic evidence corroborates landscape instability evidence. However, sediments do not rain down everywhere simultaneously (Ager, 1993). Rather, sedimentation is mostly a lateral precess, building out from a point sideways. As a result, deposits like the Organ unit are diachronous. Even though Organ sedimentation may have started about 7000 years B.P., some areas were probably not buried until later in the middle Holocene or late Holocene. Geomorphic mapping in the Desert Project indicates that the bulk of Organ alluviation occurred between 6400 and 2200 years B.P. (Gile et al., 1981).

5.5.2. Fossil pollen

Hall (1985) reviewed pollen studies in the southwestern United States. His review provides a general picture of shrinking woodlands beginning in the Late

Pleistocene and culminating in the middle Holocene. Freeman (1972) conducted a study of pollen in Organ sediments at the Gardner Spring radiocarbon site (Gile and Hawley, 1968) in the Desert Project east of Las Cruces (site 24, Fig. 1). Like Hall (1985), Freeman described a scenario of aridity and desert shrubs in the middle Holocene which gave way to increased grasslands by the late Holocene.

The pollen–isotope comparison in this study shows: (1) increased shrubs and decreased grass corresponding to depleted $\delta^{13}C$ values and increased sedimentation on the middle piedmont slopes; and (2) minor pollen changes corresponding to minor $\delta^{13}C$ changes in the lower piedmont–playa depressions (Fig. 7). As with the accumulation of pedogenic carbonate and soil organic matter, pollen accumulation is time-transgressive. For example, a land surface would receive pollen rain until burial. On the two middle piedmont sites, the increased Cheno-Am pollen at the discontinuities probably indicates increased saltbush/shadscale (*Atriplex* spp.) shrubs before burial by Organ alluvium (Fig. 7). The increased Cheno-Am pollen remained abundant throughout Organ deposition.

In this study and other studies, Cheno-Am pollen is interpreted as an indicators of desert scrub vegetation (Brown, 1982; Gish, 1993). This interpretation corroborates the onset of Organ alluviation. However, *Atriplex* spp., a component of the Cheno-Am taxon, are C_4 plants, not C_3 like other desert shrubs in the study area. Therefore, the pronounced $\delta^{13}C$ shift that accompanies increased Cheno-Am pollen at sites 1 and 2 cannot be attributed to the biomass of *Atriplex* spp. specifically at those sites. One answer to this apparent contradiction might be seen in the modern desert scrub communities in the study area. These modern scrub communities are dominated by creosote, mesquite, and tarbush, which in contrast to the *Atriplex* spp. are not prolific wind-pollinated plants (Horowitz, 1992). A similar setting might have occurred at the onset of Organ alluviation, where the biomass was dominated by insect-pollinated C_3 desert scrub with minor amounts of copious pollen producing Cheno-Am taxa.

5.5.3. Comparison to packrat midden evidence

Packrat middens provide an assemblage of plant macrofossils from rock shelters that can be radiocarbon-dated to reconstruct paleoenvironments (Betancourt et al., 1990). Most of the packrat midden research in the Chihuahuan Desert has been conducted by Van Devender (e.g., Van Devender, 1990). In the study area, two sites have been investigated: Bishop's Cap and Hueco Mountains (sites 21 and 22, Fig. 1). The Bishop's Cap site is in the southern Organ Mountains and contains a record from 43,300 years B.P. in the middle Wisconsinan to 10,300 years B.P. near the beginning of the early Holocene. Because of its age, the Bishop Cap lacks information about Holocene conditions. The Hueco Mountain site, however, does contain Holocene samples. The Hueco Site occurs across the basin floor about 65 km east of Bishop's Cap (site 22, Fig. 1). Van Devender (1990) summarized the Hueco packrat midden data as follows. Plant fossils indicate that a pinyon–juniper–oak woodland grew in the area throughout the middle and late Wisconsinan, from 42,000 to 10,800 years B.P. After 10,800 years B.P, pinyons disappeared but oaks and junipers persisted through the early Holocene until about 8000 years B.P., when oaks disappeared. At this time, honey mesquite and prickly pear appeared in a gradual transition to desert grassland. The shift to modern desert scrub conditions was completed before 3600 years B.P., about the time creosotebush appears at 3700 years B.P.

For isotope comparison, site 16 was chosen because it was a middle piedmont slope site containing buried soils close to an area containing packrat data. The pedon at site 16 consists of three deposits: Organ, Isaacks' Ranch, and Jornada II (Fig. 3). Three dating methods were attempted at this site: optically stimulated luminescence (OSL), C-14 dating of soil organic matter, and C-14 dating of soil carbonate. Only the soil carbonates yielded ages because there was too little soil organic matter for radiocarbon dating and because mineral grains were not bleached sufficiently for OSL dating. Similar to the middle piedmont sites formed in igneous alluvium, a major shift in δ^{13}C values suggest a change from C_4-dominated flora to C_3-dominated flora prior to Organ deposition (Fig. 3).

The exact timing of the isotopic shift and Organ alluviation at site 16 is uncertain. If the isotopic shift and Organ deposition occurred about 7000 years B.P., then the erosion and isotopic evidence contradict the packrat evidence for the development of desert grasslands in the middle Holocene. If, however, the isotopic shift and Organ deposition occurred at about 4000 years B.P., they corroborate packrat evidence for the development of desert scrub near the beginning of the late Holocene. At present, more research is needed to determine the timing of these events. In southern Arizona, however, Liu et al. (1996) also find isotopic evidence for desert scrub in the middle Holocene rather than the establishment of grassland as interpreted from regional packrat middens. They consider the discrepancy as possibly resulting because: (1) packrat middens are biased toward hillslope or canyon habitats; and (2) packrat foraging habits are biased toward shrub and woodland species rather than grass species.

6. Summary and conclusions

At least seven allostratigraphic units bound by discontinuities occur in the study region. One of the youngest and most extensive is the Organ unit. Organ is characterized by its weak soil profile development, stage I filaments, and lowest geomorphic position graded close to the modern arroyo levels (Ruhe, 1967; Gile et al., 1981). Based on radiocarbon-dated charcoal, the bulk of Organ alluvium was deposited between 6400 and 2200 years B.P.

On the middle piedmont slopes, major $\delta^{13}C$ shifts from as high as $-0.6‰$ to as low as $-11.1‰$ occur across discontinuities separating Organ from underlying, more highly developed soils. The isotopic shift across these discontinuities suggests a change from a C_4-dominated plant community to a C_3-dominated plant community. Although a shift from C_4 to C_3 plants can indicate a change from dry–hot to humid–cool conditions (e.g., Quade et al., 1989b; Smith et al., 1993; Mack et al., 1994), this shift can also indicate a change from mesic to aridic conditions because most desert scrub species are C_3. Because the $\delta^{13}C$ shift preceded Organ alluviation, the C_4 to C_3 shift suggests a change from grasses to desert shrubs. Pollen from middle piedmont sites also indicate that increased desert scrub vegetation accompanied Organ alluviation.

Packrat midden data for the study area indicate a four-step vegetation sequence, which in general can be summarized as follows:

(1) late Wisconsinan = pinyon–juniper–oak woodland;

(2) early Holocene = oak–juniper woodland;

(3) middle Holocene = desert grassland; and

(4) late Holocene = Chihuahuan desert scrub (Van Devender, 1990).

The $\delta^{13}C$ data from the middle piedmont soils, however, might suggest two possible differences. First, $\delta^{13}C$ values from stages II, III, and IV carbonate in buried Isaacks' Ranch and Jornada II soils are general greater than $-4‰$, suggesting a high proportion of C_4 grasses. Because carbonate in these soils formed largely in the Late Pleistocene and early Holocene (Gile et al., 1981), these times may have had more grasses than suggested by the packrat midden record, especially soils of broads alluvial plains away from rock outcrops. Second, the decline in C_4 biomass that accompanied Organ alluviation, suggests diminished grasses and increased desert scrub (Cole and Monger, 1994). If the timing of Organ alluviation and the $\delta^{13}C$ shift occurred around the beginning of the middle Holocene (Gile et al., 1981), then the middle Holocene might have been a time of desert scrub development, rather than grassland development.

$\delta^{13}C$ values were more variable than $\delta^{18}O$ values. The large $\delta^{13}C$ shifts that occurred across discontinuities separating Organ alluvium from buried soils were not accompanied by $\delta^{18}O$ shifts of similar magnitude. Of the three landform categories in this study, $\delta^{13}C$ and fossil pollen changes were greater on middle piedmont slopes. This might indicate that the middle piedmont is an environment where vegetation is more vulnerable to climate change than lower landforms that receive runoff and have finer-textured soils.

Acknowledgements

This research was supported primarily by the Department of Defense, Environmental Management Office, Fort Bliss, Texas. D. Cole was sponsored by the Geoscience Research Program, Office of Basic Energy Sciences, USDOE under contract DE-AC05-96OR22464 with Lockheed Martin Energy Research Corporation. Isotopes from the Hueco Mountain site were analyzed by Andrew Campbell, New Mexico Tech University. Contributions of Human Systems Research and the New Mexico State University Agricultural Experiment Station are very much appreciated. We thank Oliver Chadwick, Lee Nordt, Ronald Amundson, Leland H. Gile, Ann Ramenofsky, and an anonymous reviewer for valuable comments on earlier versions of the manuscript.

References

Abrahams, A.D., Parsons, A.J., Wainwright, J., 1995. Controls and determination of resistance to overland flow on semiarid hillslopes, Walnut Gulch. J. Soil Water Conserv. 50, 457–460.

Ager, D.V., 1993. The nature of the stratigraphic record. John Wiley, New York, 151 pp.

Allred, K., 1988. A field guide to the flora of the Jornada Plain. N.M., State Univ. Agric. Exp. Stn. Bull. 739, 145 pp.

Amundson, R.G., Chadwick, O.A., Sowers, J.M., Doner, H.E., 1989. The stable isotope chemistry of pedogenic carbonates at Kyle Canyon, Nevada. Soil Sci. Soc. Am. J. 53, 210–210.

Amundson, R.G., Wang, Y., Chadwick, O., Trumbore, S., McFadden, L., McDonald, E., Wells, S., DeNiro, M., 1994. Factors and processes governing the ^{14}C content of carbonate in desert soils. Earth Planet. Sci. Lett. 125, 385–405.

Amundson, R., Chadwick, O., Kendall, C., Wang, Y., DeNiro, M., 1996. Isotopic evidence for shifts in atmospheric circulation patterns during the late Quaternary in mid-North America. Geology 24, 23–26.

Antevs, E., 1955. Geologic-climate dating in the West. Am. Antiq. 20, 317–335.

Betancourt, J.L., Van Devender, T.R., Martin, P.S., 1990. Introduction. In: Betancourt, J.L., Van Devender, T.R., Martin, P.S. (Eds.), Packrat Middens: The Last 40,000 Years of Biotic Change. Univ. of Arizona Press, Tucson, pp. 2–13.

Blair, T.C., Clark, J.S., Wells, S.G., 1990. Quaternary continental stratigraphy, landscape evolution, and application to archaeology: Jarilla piedmont and Tularosa graben floor, White Sands Missile Range, New Mexico. Geol. Soc. Am. Bull. 102, 749–759.

Boutton, T.W., 1991. Stable carbon isotope ratios of natural materials, II. Atmospheric, terrestrial, marine, and freshwater environments. In: Coleman, C., Fry, B. (Eds.), Carbon Isotope Techniques. Academic Press, New York, pp. 173–186.

Brown, D.E., 1982. Biotic communities of the American Southwest-United States and Mexico. Desert Plants 4, 1–4.

Bull, W.B., 1991. Geomorphic Responses to Climatic Change. Oxford Univ. Press, New York, 326 pp.

Butler, B.E., 1959. Periodic phenomena in landscapes as a basis for soil studies. Commonwealth Scientific and Industrial Research Organization, Melbourne, Soil Publ. 14, 20 pp.

Carmichael, D.L., 1986. Archaeological Survey in the Southern Tularosa Basin of New Mexico. Historic and Natural Resources Rep. 3, Fort Bliss, TX, 404 pp.

Cerling, T.E., 1984. The stable isotopic composition of modern soil carbonate and its relationship to climate. Earth Planet. Sci. Lett. 71, 229–240.

Cerling, T.E., Quade, J., 1993. Stable carbon and oxygen isotopes in soil carbonates. In: Swart, P.K., Lohmann, K.C., McKenzie, J., Savin, S. (Eds.), Climate Change in Continental Isotopic Records. AGU, Geophys. Monogr. 78, 217–231.

Cerling, T.E., Quade, J., Wang, Y., Bowman, J.R., 1989. Carbon isotopes in soils and palaeosols as ecology and palaeoecology indicators. Nature 341, 138–139.

Cole, D.R., Monger, H.C., 1994. Influence of atmospheric CO_2 on the decline of C_4 plants during the last deglaciation. Nature 368, 533–536.

Dansgaard, W., 1964. Stable isotopes in precipitation. Tellus 16, 436–468.

Dick-Peddie, W.A., 1993. New Mexico Vegetation: Past, Present, and Future. Univ. of New Mexico Press, Albuquerque, 244 pp.

Dorn, R.I., 1994. The role of climate change in alluvial fan development. In: Abrahams, A.D., Parsons, A.J. (Eds.), Geomorphology of Desert Environments. Chapman and Hall, London, pp. 593–615.

Ehleringer, J.R., 1989. Carbon isotope ratios and physiological processes in aridland plants. In: Rundel, P.W., Ehleringer, J.R., Nagy, K.A. (Eds.), Stable Isotopes in Ecological Research. Ecological Studies Vol. 68, Springer-Verlag, New York, pp. 41–54.

Fenneman, N.M., 1931. Physiography of the Western United States. McGraw-Hill, New York, 534 pp.

Freeman, C.E., 1972. Pollen study of some Holocene alluvial deposits in Dona Ana County, Southern New Mexico. Tex. J. Sci. 24, 203–220.

Gardner, L.R., 1984. Carbon and oxygen isotope composition of pedogenic $CaCO_3$ from soil profiles in Nevada and New Mexico, U.S.A. Isot. Geosci. 2, 55–73.

Gile, L.H., 1961. A classification of ca. horizons in the soils of a desert region, Dona Ana County, New Mexico. Soil Sci. Soc. Am. Proc. 25, 52–61.

Gile, L.H., 1966. Coppice dunes and the Rotura soil. Soil Sci. Soc. Am. Proc. 30, 657–660.

Gile, L.H., 1975. Holocene soils and soil–geomorphic relations in an arid region of southern New Mexico. Quat. Res. 5, 321–360.

Gile, L.H., 1995. Pedogenic carbonate in soils of the Isaacks' Ranch surface, southern New Mexico. Soil Sci. Soc. Am. J. 59, 501–508.

Gile, L.H., Grossman, R.B., 1979. The Desert Project soil monograph. National Technical Information Service, Springfield, VA, Doc. No. PB80-135304.

Gile, L.H., Hawley, J.W., 1966. Periodic sedimentation and soil formation on an alluvial-fan piedmont in southern New Mexico. Soil Sci. Soc. Am. Proc. 30, 261–268.

Gile, L.H., Hawley, J.W., 1968. Age and comparative development of desert soils at the Gardner Spring radiocarbon site, New Mexico. Soil Sci. Soc. Am. Proc. 32, 709–719.

Gile, L.H., Peterson, F.F., Grossman, R.B., 1965. The K horizon—a master soil horizon of carbonate accumulation. Soil Sci. 99, 74–82.

Gile, L.H., Peterson, F.F., Grossman, R.B., 1966. Morphological and genetic sequences of carbonate accumulation in desert soils. Soil Sci. 101, 347–360.

Gile, L.H., Hawley, J.W., Grossman, R.B., 1981. Soils and geomorphology in the Basin and Range area of southern New Mexico—Guidebook to the Desert Project. N.M., Bur. Mines Miner. Resour. Mem. 39, 222 pp.

Gish, J.W., 1979. Palynology research at Pueblo Grande Ruin. Kiva 44, 159–172.

Gish, J.W., 1993. Pollen results from three study localities on Fort Bliss Military Reservation, New Mexico. In: Monger, H.C. (Ed.), Soil–Geomorphic and Paleoclimatic Characteristics of the Fort Bliss Maneuver Areas, Southern New Mexico and Western Texas. Historic and Natural Resources, Fort Bliss, TX, Rep. 10, pp. 93–116.

Grootes, P.M., 1993. Interpreting continental oxygen isotope records. In: Swart, P.K., Lohmann, K.C., McKenzie, J., Savin, S. (Eds.), Climate Change in Continental Isotopic Records. AGU, Geophys. Monogr. 78, 37–46.

Grossman, R.B., Ahrens, R.J., Gile, L.H., Montoya, C.E., Chadwick, O.A., 1995. Areal evaluation of organic and carbonate carbon in a desert area of southern New Mexico. In: Lal, R., Kimble, J., Livine, E., Stewart, B.A. (Eds.), Soils and Global Change. CRC Press, London, pp. 81–92.

Guthrie, R.L., Witty, J.E., 1982. New designations for soil horizons and layers and the new Soil Survey Manual. Soil Sci. Soc. Am. J. 46, 443–444.

Hall, S.A., 1985. Quaternary pollen analysis and vegetational history of the Southwest. In: Bryant, V.M. Jr., Holloway, R.G. (Eds.), Pollen Records of Late Quaternary North American Sediments. American Association of Stratigraphic Palynologists Foundation, Dallas, TX, pp. 95–124.

Hawley, J.W., 1975a. Quaternary history of Dona Ana County region, South-central New Mexico. In: Seager, W.R., Clemons, R.E., Callender, J.F. (Eds.), New Mexico Geological Society Guidebook, 26th Field Conference, Las Cruces Country. New Mexico Bureau of Mines and Mineral Resources, Socorro, pp. 139–150.

Hawley, J.W., 1975b. The Desert Soil–Geomorphology Project. In: Seager, W.R., Clemons, R.E., Callender, J.F. (Eds.), New Mexico Geological Society Guidebook, 26th Field Conference, Las Cruces Country. New Mexico Bureau of Mines and Mineral Resources, Socorro, pp. 183–186.

Hawley, J.W., 1993. Geomorphic setting and late Quaternary history of pluvial-lake basins in the southern New Mexico Region. N.M., Bur. Mines Miner. Resour. Open-File Rep. 391, 28 pp.

Hawley, J.W., Kottlowski, F.E., 1969. Quaternary geology of the south-central New Mexico border region. In: Kottlowski, F.E., LeMone, D.V. (Eds.), Border Stratigraphy Symposium. N.M., Bur. Mines Miner. Resour. Circ. 104, 89–115.

Hawley, J.W., Bachman, G.O., Manley, K., 1976. Quaternary stratigraphy in the Basin and Range and Great Plains provinces, New Mexico and western Texas. In: Mahaney, W.C. (Ed.), Quaternary Stratigraphy of North America. Dowden, Hutchinson, and Ross, Stroudsburg, PA, pp. 235–274.

Hays, P.D., Grossman, E.L., 1991. Oxygen isotopes in meteoric calcite cements as indicators of continental paleoclimate. Geology 19, 441–444.

Horowitz, A., 1992. Palynology of Arid Lands. Elsevier, Amsterdam, 546 pp.

Kelly, E.F., Yonker, C., Marino, B., 1993. Stable carbon isotope composition of paleosols: An application to Holocene. In: Swart, P.K., Lohmann, K.C., McKenzie, J., Savin, S. (Eds.), Climate Change in Continental Isotopic Records. AGU, Geophys. Monogr. 78, 233–239.

King, W.E., Hawley, J.W., 1975. Geology and ground-water resources of the Las Cruces area. In: Seager, W.R., Clemons, R.E., Callender, J.F. (Eds.), New Mexico Geological Society Guidebook, 26th Field Conference, Las Cruces Country. New Mexico Bureau of Mines and Mineral Resources, Socorro, pp. 195–204.

Liu, B., Phillips, F., Hoines, S., Campbell, A.R., Sharma, P., 1995. Water movement in desert soil traced by hydrogen and oxygen isotopes, chloride, and chlorine-36, southern Arizona. J. Hydrol. 168, 91–110.

Liu, B., Phillips, F.M., Campbell, A.R., 1996. Stable carbon and oxygen isotopes of pedogenic carbonates, Ajo Mountains, southern Arizona: Implications for paleoenvironmental change. Palaeogeogr., Palaeoclimatol., Palaeoecol. 124, 233–246.

Mack, G.H., Salyards, S., James, W.C., 1993. Magnetostratigraphy of the Plio-Pleistocene Camp Rice and Palomas formations in the Rio Grande Rift of southern New Mexico. Am. J. Sci. 293, 49–77.

Mack, G.H., Cole, D.R., James, W.C., Giordano, T.H., Salyards, S.L., 1994. Stable oxygen and carbon isotopes of pedogenic carbonate as indicators of Plio-Pleistocene paleoclimate in the southern Rio Grande Rift, South-Central New Mexico. Am. J. Sci. 294, 621–640.

Mack, G.H., McIntosh, W.C., Leeder, M.R., Monger, H.C., 1996. Plio-Pleistocene pumice floods in the ancestral Rio Grande, southern Rio Grande rift, USA. Sediment. Geol. 103, 1–8.

Mauldin, R.P., 1995. Groping for the Past: Investigating Archaeological Patterns across Space and Time in the Southern Southwestern United States. Unpubl. Dissertation, Univ. of New Mexico, Albuquerque, 381 pp.

McDonald, E.V., Busacca, A.J., 1990. Interaction between aggradating geomorphic surfaces and the formation of a late Pleistocene paleosol in the Pallouse loess of eastern Washington state. Geomorphology 3, 449–470.

McLean, J.S., 1975. Saline ground water in the Tularosa Basin, New Mexico. In: Seager, W.R., Clemons, R.E., Callender, J.F. (Eds.), New Mexico Geological Society Guidebook, 26th Field Conference, Las Cruces Country. New Mexico Bureau of Mines and Mineral Resources, Socorro, pp. 237–238.

Monger, H.C., 1993. Soil–geomorphic and paleoclimatic characteristics of the Fort Bliss maneuver areas, southern New Mexico and western Texas. Historic and Natural Resources, Fort Bliss, TX, Rep. 10, 213 pp.

Monger, H.C., 1995. Pedology in arid lands archaeological research: An example from southern New Mexico—western Texas. In: Collins, M. (Ed.), Pedological Perspectives in Archeological Research. Soil Sci. Soc. Am. Spec. Publ. 44, 35–50.

Monger, H.C., Daugherty, L.A., 1991a. Pressure solution: possible mechanism for silicate grain dissolution in a petrocalcic horizon. Soil Sci. Soc. Am. J. 55, 1625–1629.

Monger, H.C., Daugherty, L.A., 1991b. Neoformation of palygorskite in a southern New Mexico Aridisol. Soil Sci. Soc. Am. J. 55, 1646–1650.

Monger, H.C., Daugherty, L.A., Lindemann, W.C., Liddell, C.M., 1991a. Microbial precipitation of pedogenic calcite. Geology 19, 997–1000.

Monger, H.C., Daugherty, L.A., Gile, L.H., 1991b. A microscopic examination of pedogenic calcite in an Aridisol of southern New Mexico. In: Nettleton, W.D. (Ed.), Occurrence, Characteristics, and Genesis of Carbonate, Gypsum, and Silica Accumulations in Soils. Soil Sci. Soc. Am. Spec. Publ. 26, 37–60.

Nordt, L.C., Wilding, L.P., Hallmark, C.T., Jacob, J.S., 1996. Stable carbon isotope composition of pedogenic carbonates and their use in studying pedogenesis. In: Boutton T.W., Yamasaki, S. (Eds.), Mass Spectrometry of Soils. Marcel Dekker, New York, pp. 133–154.

Pendall, E.G., Harden, J.W., Trumbore, S.E., Chadwick, O.A., 1994. Isotopic approach to soil carbonate dynamics and implications for paleoclimatic interpretations. Quat. Res. 42, 60–71.

Peterson, F.F., 1981. Landforms of the Basin and Range Province defined for Soil Survey. Nevada Agricultural Experiment Station, Tech. Bull. 28, Univ. of Nevada, Reno, 52 pp.

Peterson, F.F., Bell, J.W., Dorn, R.I., Ramelli, A.R., Ku, T.L., 1995. Late Quaternary geomorphology and soils in Crater Flat, Yucca Mountain area, southern Nevada. Geol Soc. Am. Bull. 107, 379–395.

Quade, J., Cerling, T.E., Bowman, J.R., 1989a. Systematic variations in carbon and oxygen isotopic composition of pedogenic carbonate along elevation transects in the southern Great Basin, United States. Geol. Soc. Am. Bull. 101, 464–475.

Quade, J., Cerling, T.E., Bowman, J.R., 1989b. Development of Asian monsoon revealed by marked ecological shift during the latest Miocene in northern Pakistan. Nature 342, 163–166.

Rabenhorst, M.C., Wilding, L.P., West, L.T., 1984. Identification of pedogenic carbonates using stable isotopic and microfabric analysis. Soil Sci. Soc. Am. J. 48, 125–132.

Rozanski, K., Araguas-Araguas, L., Gonfiantini, R., 1993. Isotopic patterns in modern global precipitation. In: Swart, P.K., Lohmann, K.C., McKenzie, J., Savin, S. (Eds.), Climate Change in Continental Isotopic Records. AGU, Geophys. Monogr. 78, 1–36.

Ruhe, R.V., 1964. Landscape morphology and alluvial deposits in southern New Mexico. Ann. Assoc. Am. Geogr. 54, 147–159.

Ruhe, R.V., 1967. Geomorphic surfaces and surficial deposits in southern New Mexico. N.M., Bur. Mines Miner. Resour. Mem. 18, 65 pp.

Schlesinger, W.H., Marino, G.M., Fonteyn, P.J., 1989. Stable isotope ratios and the dynamics of caliche in desert soils. In: Rundel, P.W., Ehleringer, J.R., Nagy, K.A. (Eds.), Stable Isotopes in Ecological Research. Ecological Studies Vol. 68, Springer-Verlag, New York, pp. 309–317.

Schlesinger, W.H., Reynolds, J.F., Cunningham, G.L., Huenneke, L.F., Jarrell, W.M., Virginia, R.A., Whitford, W.G., 1990. Biological feedbacks in global desertification. Science 247, 1043–1048.

Schmidt, R.H., 1979. A climatic delineation of the 'real' Chihuahuan Desert. J. Arid Environ. 2, 243–250.

Seager, W.R., 1981. Geology of Organ Mountains and southern San Andres Mountains, New Mexico. N.M., Bur. Mines Miner. Resour. Mem. 36, 97 pp.

Seager, W.R., Hawley, J.W., Kottlowski, F.F., Kelley, S.A., 1987. Geology of the east half of Las Cruces and northeast El Paso $1° \times 2°$ sheets, New Mexico. N.M., Bur. Mines Miner. Resour., Geol. Map 57.

Smith, G.A., Wang, Y., Cerling, T.E., Geissman, J.W., 1993. Comparison of paleosol-carbonate isotope record to other records of Pliocene–early Pleistocene climate in the western United States. Geology 21, 691–694.

Spaulding, W.G., 1991. A middle Holocene vegetation record from the Mojave Desert of North America and its paleoclimatic significance. Quat. Res. 35, 427–437.

Syvertsen, J.P., Nickell, G.L., Spellenberg, R.W., Cunningham, G.L., 1976. Carbon reduction pathways and standing crop in three Chihuahuan Desert plant communities. Southwest Nat. 21, 311–320.

Van Devender, T.R., 1990. Late Quaternary vegetation and climate of the Chihuahuan Desert, United States and Mexico. In: Betancourt, J.L., Van Devender, T.R., Martin, P.S. (Eds.), Packrat Middens: The last 40,000 years of biotic change. Univ. of Arizona Press, Tucson, pp. 104–133.

Wang, Y., Amundson, R., Trumbore, S., 1994. A model for soil $^{14}CO_2$ and its implications for using ^{14}C to date pedogenic carbonate. Geochim. Cosmochim. Acta 58, 393–399.

Wang, Y., McDonald, E., Amundson, R., McFadden, L., Chadwick, O., 1996. An isotopic study of soils in chronological sequences of alluvial deposits, Providence Mountains, California. Geol. Soc. Am. Bull. 108, 379–391.

Waters, M.R., 1989. Late Quaternary lacustrine history and paleoclimatic significance of pluvial Lake Cochise, southeastern Arizona. Quat. Res. 31, 1–11.

York, J.C., Dick-Peddie, W.A., 1969. Vegetation changes in southern New Mexico during the past hundred years. In: McGinnies, W.G., Goldman, B.J. (Eds.), Arid Lands in Perspective. Univ. of Arizona Press, Tucson, pp. 155–166.

Yurtsever, Y., Gat, J.R., 1981. Atmospheric waters. In: Gat, J.R., Gonfiantini, R. (Eds), Stable Isotope Hydrology, Deuterium and Oxygen-18 in the Water Cycle. IAEA Vienna, Tech. Rep. Ser. 210, pp. 103–142.